

Screen of Pseudopeptidic Inhibitors of Human Sirtuins 1–3: Two Lead Compounds with Antiproliferative Effects in Cancer Cells

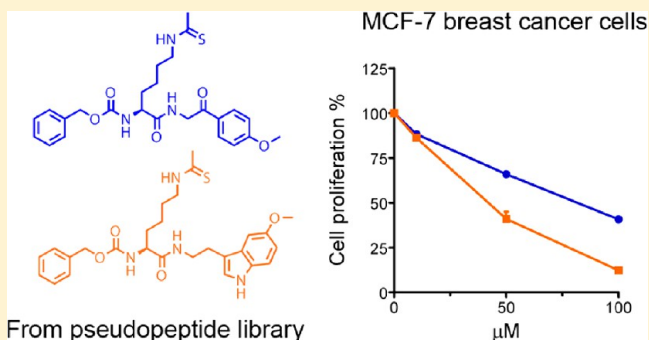
Paolo Mellini,^{†,§} Tarja Kokkola,[†] Tiina Suuronen,^{||} Heikki S. Salo,[†] Laura Tolvanen,[†] Antonello Mai,[§] Maija Lahtela-Kakkonen,[†] and Elina M. Jarho^{*,†}

[†]School of Pharmacy and ^{||}Department of Neurology, Institute of Clinical Medicine, University of Eastern Finland, P.O. Box 1627, 70211 Kuopio, Finland

[§]Istituto Pasteur - Fondazione Cenci Bolognetti, Dipartimento di Chimica e Tecnologie del Farmaco, Università degli Studi di Roma "La Sapienza", P.le A. Moro 5, 00185 Rome, Italy

S Supporting Information

ABSTRACT: In the past few years sirtuins have gained growing attention for their involvement in many biological processes such as cellular metabolism, apoptosis, aging and inflammation. In this contribution, we report the synthesis of a library of thioacetylated pseudopeptides that were screened against human sirtuins 1–3 to reveal their *in vitro* inhibition activities. Molecular modeling studies were performed to acquire data about the binding modes of the inhibitors. Three sirtuin inhibitors were subjected to cellular studies, and all of them showed an increase in acetylation of Lys382 of p53 after DNA damage. Furthermore, two of the compounds were able to inhibit both A549 lung carcinoma and MCF-7 breast carcinoma cell growth in micromolar concentration with the ability to arrest cancer cell cycle in the G₁ phase.



INTRODUCTION

The reversible protein acetylation status plays an important role in the regulatory mechanisms that control the function of histone and nonhistone proteins. The class III histone deacetylases, also called sirtuins (SIRT1–7),¹ characterized by a conserved 270 amino acid catalytic core domain, are NAD⁺ dependent enzymes able to catalyze substrate-specific deacetylase (SIRT1–3, and 6) and ADP ribosyltransferase² (SIRT4 and 6) reactions. Furthermore, it has recently been found that SIRT5 has potent demalonylase and desuccinylase enzymatic activity.^{3,4} Sirtuins are able to deacetylate a variety of histone (H1, H3, H4) and nonhistone targets such as PGC-1 α , LXR, FOXO, NF- κ B, p53, p73, p300, α -tubulin, AceCS1 and AceCS2.^{5,6} They also show different cellular localizations, SIRT1, SIRT6, and SIRT7 being nuclear, SIRT2 cytoplasmic and SIRT3–5 mitochondrial. Due to this it has been widely shown that the activity of sirtuins is involved in the cellular metabolism regulation, neuroprotection, apoptosis, inflammation, cell survival/aging, telomere maintenance etc.^{7–10} SIRT1 has gained considerable attention for its debated activity in tumor progression,⁷ in which it can act as a potential tumor suppressor or as an oncogene. Indeed, it has been reported that SIRT1 can be upregulated in many cancer types such as human prostate cancer,^{11,12} acute myeloid leukemia,¹³ adult T-cell lymphoma,¹⁴ colon cancer,¹⁵ breast cancer¹⁶ and lung cancer,¹⁷ in which SIRT1 can probably promote the cancer development via the inactivation of a number of proteins, such as p53 and

FOXO, associated with tumor suppression.¹⁸ SIRT2 has also been suggested to play a role in tumorigenesis through its inhibitory effects on p53.¹⁹ Furthermore, recently Alhazzazi and co-workers showed that SIRT3 is overexpressed in OSCC (oral squamous cell carcinoma) *in vitro* and *in vivo* and its down-regulation reduced tumor burden *in vivo*.²⁰ Lately, it has been suggested that targeting both SIRT1 and SIRT2 could be a powerful approach in cancer therapy.^{21–24}

The thioacetylated peptidic inhibitors have represented the first successful approach to develop potent competitive SIRT1/2 inhibitors.²⁵ The inhibition mechanism (Figure 1), elucidated by Smith and Denu, shows that, after a fast nicotinamide cleavage, the thioacetyl inhibitor is readily converted to a stalled intermediate 1'-S-alkylamide with a consequent retardation of the overall turnover rate.^{26–28}

In the scenario in which the peptidic scaffold gave compounds with potent inhibition activity^{29,30} but negligible drug-like properties, Suzuki et al.³¹ and Huhtiniemi and co-workers a few years after,³² developed novel classes of pseudopeptides with an N^ε-thioacetyl lysine residue (Chart 1) in order to improve the cell permeability.

Pursuing the versatility of the pseudopeptidic scaffold, we focused our efforts on the preparation and biological evaluation of a novel fragment-based library (Chart 2, Tables 1–3). The

Received: March 26, 2013

Published: August 8, 2013

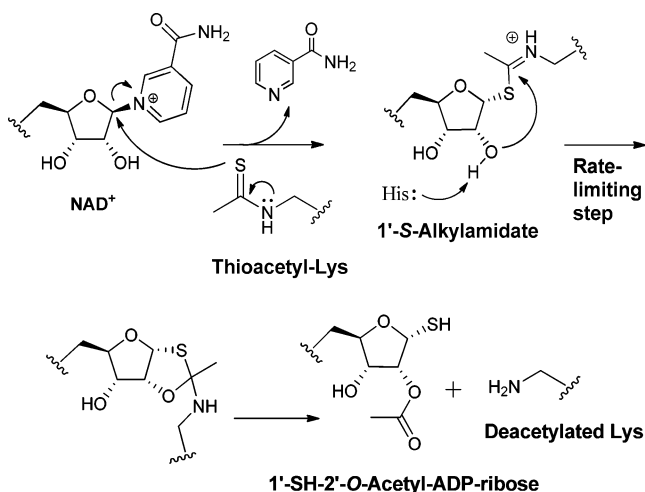


Figure 1. Mechanism of sirtuin inhibition of thioacetylated peptides.

Chart 1. Reference Compound A by Suzuki et al.³¹ and Reference Compound B by Huhtiniemi et al.³²

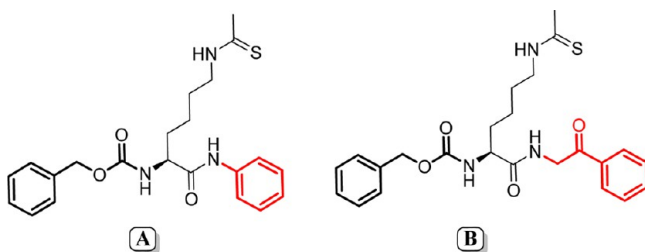
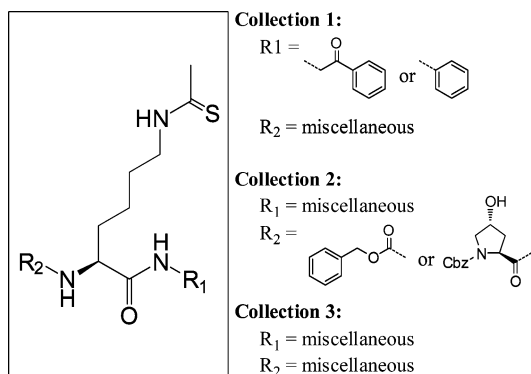


Chart 2. General Structure and the Compound Collections of the Pseudopeptide Library



library was generated considering our previously reported binding hypothesis that was developed with SIRT3 as the target structure.³² In this hypothesis, we suggested that a potential sirtuin inhibitor should create an H-bond network with Val292, Glu295, Glu296 and Glu325 (Figure 2). In addition, in the N-terminal area of a pseudopeptidic compound the binding affinity could be improved by formation of a H-bond to Leu298 and filling the cavity surrounded by residues Pro297, Leu298, Phe302 and Leu303. On the other hand, in the C-terminal a compound with aromatic interactions with Phe294 or a H-bond with Glu325 might have good inhibition potency.

To improve the knowledge of pseudopeptidic interactions in various sirtuins and to get structure–activity relationship (SAR) data, a set of novel pseudopeptides was designed. A small library of 30 compounds was synthesized (Chart 2, Tables

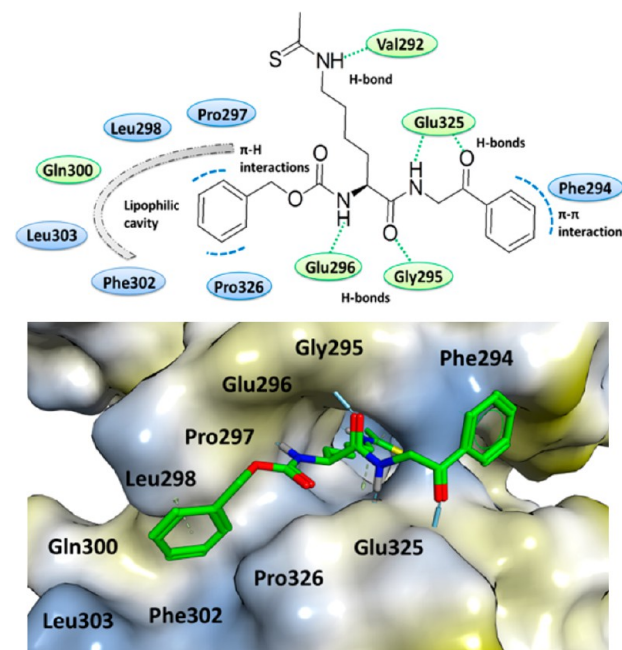
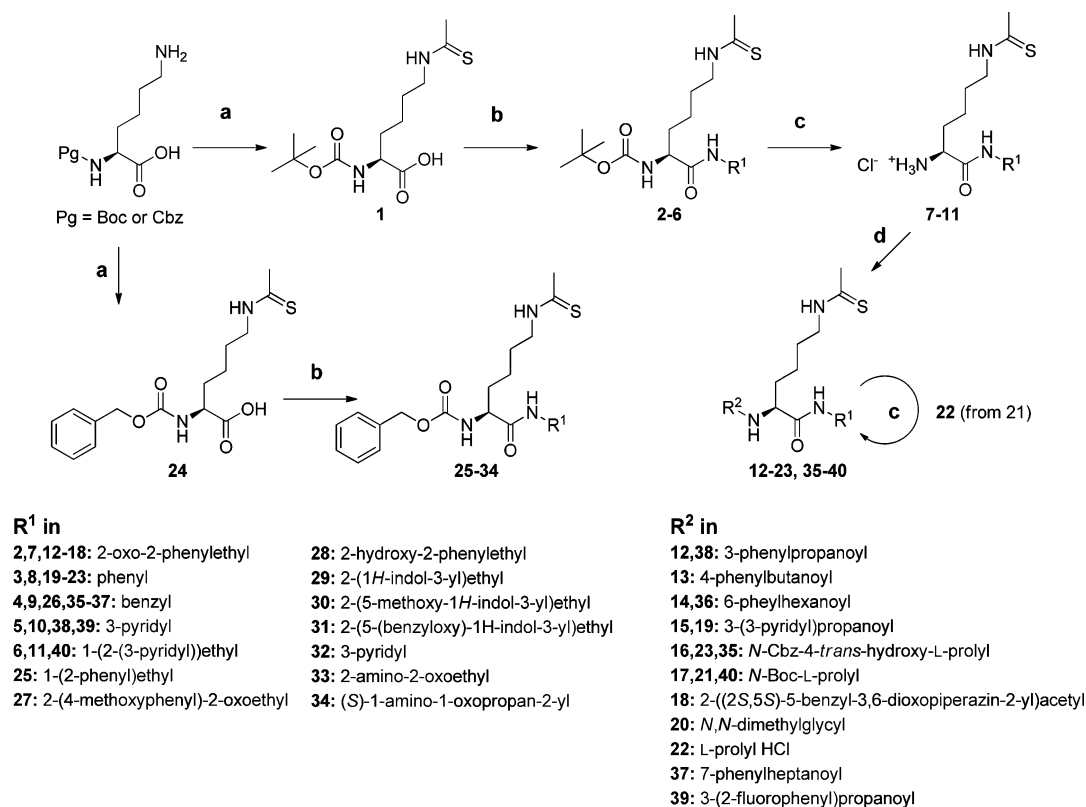


Figure 2. Scheme of the interaction pattern reported for a pseudopeptidic inhibitor in SIRT3 that fulfills the binding hypothesis. In the cartoon, H-bonds and aromatic interactions are represented by dashed lines, correspondingly in green and blue.

1–3) and screened in vitro against SIRT1–3 with the aim to understand how heterogeneous N- and C-terminal modifications might induce changes in the activity. Three compounds were selected for cellular studies. All three compounds were cell-permeable and nontoxic. Furthermore, two of the compounds showed antiproliferative effects on two different cancer cell lines (A549 and MCF-7) causing cell cycle arrest at the G₁ phase.

CHEMISTRY

The synthetic pathway to compounds 1–40 is depicted in Scheme 1. The N^ε-thioacetylated derivatives 1 and 24 were synthesized using ethyl dithioacetate and EtOH/10% (w/v) Na₂CO_{3(aq)} at rt for 12 h according to the literature.^{25,32} Compounds 2–6 and 25–34 were obtained with a coupling reaction between the activated acid 1 or 24 and an appropriate amine using the coupling agent TBTU (O-(benzotriazol-1-yl)-N,N,N',N'-tetramethyluronium tetrafluoroborate) in dimethylformamide (DMF)/pyridine under argon flow. The hydrochlorides 7–11 were gained via Boc (*tert*-butoxycarbonyl) deprotection³³ performed at 60 °C using 15 equiv of HCl(aq). 12 N, 2-propanol and 1,2-ethanedithiol as a scavenger for trapping the *tert*-butyl cation generated in situ. Initially, Boc deprotection was attempted in ethyl acetate under HCl-gas flow in the absence of a scavenger in order to precipitate the product as the HCl salt from the reaction mixture. However, the ¹H-spectrum revealed the disappearance of the thioacetyl methyl singlet (2.4 ppm in DMSO-*d*₆) and showed instead a methyl singlet at 1.8 ppm, a shift characteristic of an acetyl methyl (unpublished data). Thus, the required amount of HCl was optimized; 15 equiv of HCl divided in three portions gave complete consumption of the starting material. This, together with the added scavenger, protected the thioacetyl group during the deprotection step. Compounds 12–23 and 35–40 were synthesized according to the above-mentioned coupling

Scheme 1^a

^aReagents and conditions: (a) Ethyl dithioacetate, EtOH/10% (w/v) Na₂CO_{3(aq)}, rt, 12 h; (b) appropriate amine or carboxylic acid, TBTU, DMF/pyridine (1:1), argon flow, rt, 2–3 h; (c) 2-propanol, 1,2-ethanedithiol, HCl_(aq) 12 N, 15 equiv, 60 °C, 2–3 h.

procedure; in this case the appropriate acid was activated with TBTU to react with the corresponding unblocked amine. The hydrochloride release of the starting material 7 was a critical step that reduced the yields of the acetophenone (i.e., 2-oxo-2-phenyl ethyl) derivatives 12–18. As a free amine, compound 7 underwent spontaneous side reactions; most likely an intramolecular cyclization between the free amino group and the ketone function responsible for generating several byproducts during the coupling step.

RESULTS AND DISCUSSION

Structure–Activity Relationship. A compound library of 30 pseudo-peptides was synthesized. One collection explored modifications in the N-terminus (Table 1), the other collection explored the modifications in the C-terminus (Table 2) and, in the third collection miscellaneous modifications at both termini were studied (Table 3). All compounds were screened in vitro against SIRT1–3 at 50 μM concentration (Tables 1–3). However, the numbering of the target protein amino acids is adopted from SIRT3 in the structure–activity discussion unless otherwise noted. The main differences between SIRT1–3 substrate binding sites are labeled in Figure 3.

The first set of compounds with modifications in the N-terminus shared a 2-oxo-2-phenylethyl moiety in the C-terminus (2, 12–18 in Table 1). These compounds fulfill the H-bonding network and the C-terminal π – π interaction requirements of the binding hypothesis (Figure 2). For SIRT1, the fulfillment of these requirements is enough to give highly potent compounds; despite the structural changes in the N-terminus, compounds 12–18 gave $\geq 95\%$ inhibition.

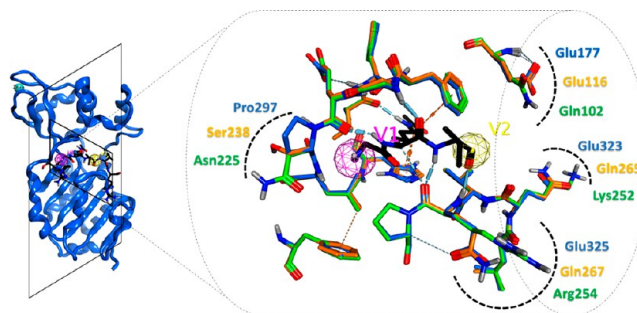


Figure 3. Overall structure of SIRT3 (PDB code: 3glr) is represented in blue ribbon (left), and shown is the superimposition of the substrate binding sites (right) of SIRT1 (green) and SIRT2 (orange) homology models and SIRT3 crystal structure (blue). The acetylated substrate is colored in black, the N- and C-terminal sides are represented by spheres V1 (pink) and V2 (yellow), respectively.

Compound 2 with the N-terminal Boc-group gave 91% SIRT1 inhibition, although weakest within this set it was still highly active. For SIRT2 and SIRT3, more variation was seen in the inhibitory activities suggesting that the optimization of the N-terminus is more critical for these enzymes. However, the C-terminal 2-oxo-2-phenylethyl moiety seems to be very good also for SIRT2 and SIRT3 because $\geq 90\%$ inhibition was achieved in several examples.

Compounds 12–14 show the same trend for all the three enzymes; elongation of the chain improved inhibitory activity, the best compound being 14 with five methylene groups between the phenyl and carbonyl functions. On the basis of the modeling studies, compound 14 seems better to be

complementary with the hydrophobic cavity compared to compounds **12** and **13**. Compound **2** with the N-terminal Boc-group gave SIRT2 inhibition comparable to compound **14** but against SIRT1 and SIRT3 it showed decreased activity. Introduction of the pyridyl group did not improve the inhibition of any of the enzymes (**15** vs **12**). Compounds **16–18** were designed to improve the N-terminal interactions in the lipophilic cavity. Modeling studies also show that the hydroxyl moiety of the 4-hydroxy-L-prolyl group in compound **16** can form an additional H-bond with Gly295 (Figure 4D).

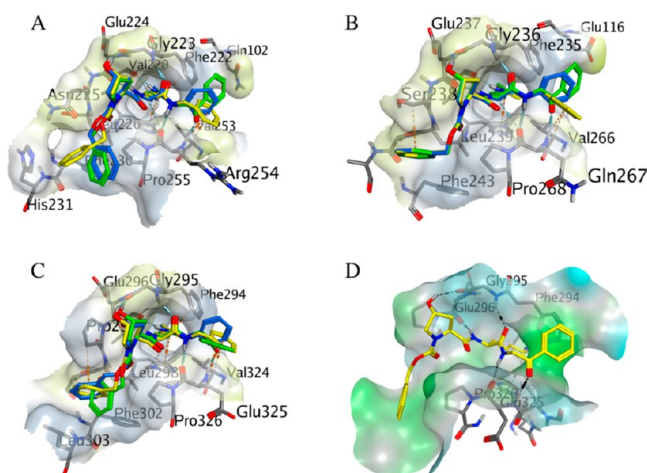


Figure 4. Docking poses for **16** (green), **23** (blue), **35** (yellow) in (A) SIRT1, (B) SIRT2, (C) SIRT3. On the protein surface the light green represents the hydrophilic, and the light blue, the lipophilic areas. (D) Compound **16** docked in SIRT3, highlighting the additional H-bond between the hydroxyl group and Gly295.

Interestingly, compound **16** was the only compound within the whole compound library that achieved $\geq 90\%$ inhibition of all three studied sirtuins and, thus, seems to possess a well-optimized structure.

The second set of compounds with modifications in the N-terminus shared a phenyl moiety in the C-terminus (**19–23** in Table 1). These compounds are missing one H-bond of the hydrogen-bonding network due to the lack of the C-terminal H-bond acceptor. Furthermore, the phenyl ring is not in the optimal position for the C-terminal π – π interaction. It is obvious that the C-terminal phenyl is not as good a structure as that of the above studied 2-oxo-2-phenylethyl moiety (**19**, **21**, **23** vs **15**, **17**, **16**, respectively).

Again, the N-terminal Cbz-4-hydroxy-L-prolyl moiety (**23**) gave the most potent compound (Figure 4). Boc-L-prolyl (**21**) instead, shows only activity comparable to that of the 3-(3-pyridyl)propanoyl fragment (**19**) in this series. Boc deprotection of **21** gave compound **22** with an L-prolyl moiety, and further simplification gave compound **20** with an N,N-dimethyl-glycine. Against SIRT1, compound **22** was able to maintain inhibition (86%), possibly due to an H-bond from the NH-proton of the L-proline to Gly223 (SIRT1 numbering). Compound **20** lacks this proton and shows decreased activity (62%). However, against SIRT2 and SIRT3 both **20** and **22** show only weak inhibition. This is in line with our previous finding with peptidic inhibitors²⁹ wherein SIRT1 can be inhibited with smaller compounds. Small pseudopeptides provide an approach to gain SIRT1 selectivity; compound **22**

Table 1. Screening of the N-Terminal Modifications

No.	R ₂	Inhibition-% @ 50 μ M ^a		
		SIRT1	SIRT2	SIRT3

2		91 \pm 0.6	87 \pm 0.5	63 \pm 1.2
12		96 \pm 0.1	65 \pm 1.5	68 \pm 3.1
13		98 \pm 0.1	76 \pm 2.3	72 \pm 0.2
14		98 \pm 0.1	83 \pm 0.4	82 \pm 0.3
15		95 \pm 0.3	58 \pm 0.6	62 \pm 1.3
16		99 \pm 0.0	96 \pm 0.3	90 \pm 0.2
17		97 \pm 0.4	95 \pm 0.5	76 \pm 1.2
18		96 \pm 0.2	73 \pm 1.2	61 \pm 0.3

19		82 \pm 0.2	39 \pm 2.6	44 \pm 0.3
20		62 \pm 2.2	18 \pm 1.1	16 \pm 1.1
21		80 \pm 0.5	44 \pm 0.5	45 \pm 2.2
22		86 \pm 0.1	13 \pm 3.1	19 \pm 0.8
23		90 \pm 0.5	54 \pm 1.4	69 \pm 1.3

^aFluor de Lys assay; values are means \pm SD of at least three experiments.

shows the highest SIRT1 selectivity among the pseudopeptide library.

The first set of compounds with modifications in the C-terminus shared a Cbz group in the N-terminus (**25–34** in Table 2). Although the C-terminal 2-oxo-2-phenylethyl moiety had proved to be a very good structure (Table 1), it was causing side reactions during the synthesis and reducing the yields. Thus, it was decided to explore whether a more stable group with similar activity could be found. The reduction (**28**) or deletion (**25**) of the carbonyl function (Figure 5) induced a uniform loss in potency, probably because of the lost H-bond to the carbonyl function. Compound **28** was tested as a mixture

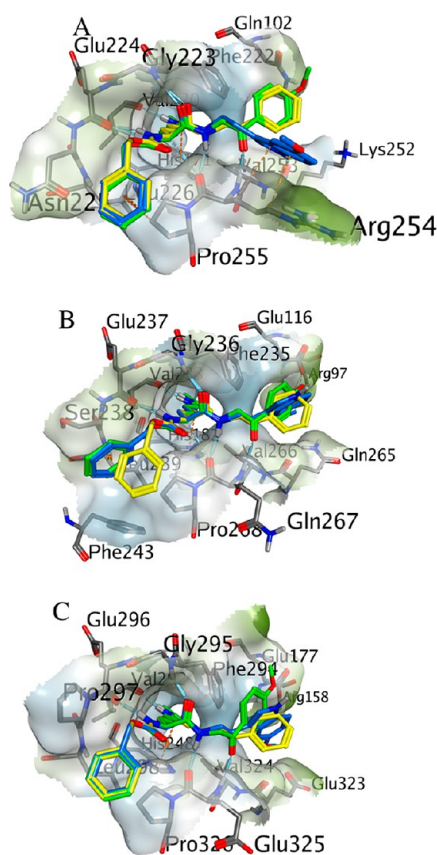


Figure 5. Docking poses for **25** (yellow), **27** (green), **30** (blue) in (A) SIRT1, (B) SIRT2, (C) SIRT3. On the protein surface the light green represents the hydrophilic, and the light blue, the lipophilic areas.

of diastereomers, but modeling did not suggest favorable interactions for one over the other. Next, the phenyl function was positioned closer to the thioacetylated lysine giving the benzyl derivative **26**. For SIRT1 and SIRT3, this optimization of the C-terminal π - π interaction could compensate for the lost H-bond, and high inhibition was observed. SIRT2 instead showed different behavior; the H-bond seems to be more crucial for the SIRT2 inhibition. These results were verified also by another set of compounds (Figure 4, Table 2); compared to compound **16**, compound **35** shows similar SIRT1 and SIRT3 inhibition but shows decreased SIRT2 inhibition. However, both of these compounds show higher inhibition compared to compound **23** with the C-terminal phenyl group.

Larger C-terminal aromatic groups were studied by compounds **27** and **29–31**. The tryptamine moiety (**29**) does not show an optimal interaction with the Phe294. However, the tryptamine can have other hydrophobic interactions with surrounding hydrophobic residues. Also, in SIRT1 there is a possibility for the tryptamine nitrogen to form an additional H-bond with Lys252 (SIRT1 numbering, compound **30** in Figure 5). Further bulkiness was gained by the methoxy (**30**) and benzyloxy (**31**) groups. These hydrophobic groups increase C-terminal hydrophobic interactions and improve potency. Also, the methoxy group in compound **27** can increase the hydrophobic interactions (Figure 5).

Three smaller, more polar C-terminal fragments were also studied. The pyridyl group in compound **32** can have a π - π interaction to the protein but surrounding water provides competing interactions to the polar moiety. Compounds **33**

Table 2. Screening of the C-Terminal Modifications

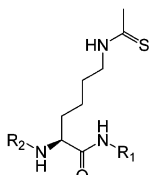
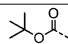
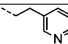
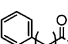
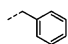
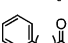
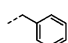
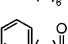
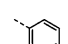
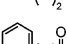
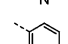

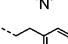
No.	R ₁	Inhibition-% @ 50 μ M ^a		
		SIRT1	SIRT2	SIRT3
Ref.A		83 \pm 0.5	81 \pm 1.1	62 \pm 1.5
Ref.B		97 \pm 0.3	94 \pm 0.3	74 \pm 0.9
25		72 \pm 3.5	52 \pm 1.6	41 \pm 1.9
26		91 \pm 0.1	67 \pm 0.6	71 \pm 2.8
27		97 \pm 0.1	97 \pm 0.2	82 \pm 1.3
28		77 \pm 0.2	54 \pm 3.1	45 \pm 2.7
29		85 \pm 0.7	61 \pm 2.3	46 \pm 3.8
30		88 \pm 0.3	66 \pm 1.1	63 \pm 1.2
31		87 \pm 0.4	79 \pm 0.6	68 \pm 2.8
32		84 \pm 1.0	70 \pm 1.3	59 \pm 1.7
33		91 \pm 0.3	72 \pm 0.5	77 \pm 0.1
34		96 \pm 0.2	86 \pm 0.2	85 \pm 0.9
16		99 \pm 0.0	96 \pm 0.3	90 \pm 0.2
23		90 \pm 0.5	54 \pm 1.4	69 \pm 1.3
35		97 \pm 0.2	87 \pm 0.7	93 \pm 0.1

^aFluor de Lys assay; values are means \pm SD of at least three experiments.

and **34** lack an aromatic ring and cannot form π - π interactions. However, these compounds are able to retain a good inhibition potency which may be due to an additional H-bond to the terminal amide nitrogen. The stereochemistry of the chiral compound **34** apparently orientates the H-bonding more properly.

A pyridyl group is often used to improve water solubility of compounds. Therefore, C-terminal pyridyl moieties were combined to miscellaneous N-terminal fragments (Table 3). Compounds **6** and **40** with the C-terminal 2-(3-pyridyl)ethyl fragment show weak to moderate sirtuin inhibition. Compounds **38** and **39** possess the C-terminal 3-pyridyl moiety. In

Table 3. Screening of the Miscellaneous Modifications

Structure	No.	R ₂	R ₁	Inhibition-% @ 50 μ M ^a		
				SIRT1	SIRT2	SIRT3
	6			41 \pm 1.9	28 \pm 3.8	24 \pm 0.3
	36			100 \pm 0.1	71 \pm 0.6	84 \pm 0.2
	37			99 \pm 0.2	74 \pm 1.2	87 \pm 0.3
	38			83 \pm 1.0	21 \pm 3.4	39 \pm 1.2
	39			94 \pm 0.4	74 \pm 0.2	72 \pm 0.6
	40			66 \pm 0.5	49 \pm 1.1	68 \pm 3.0

^aFluor de Lys assay; values are means \pm SD of at least three experiments.

Table 4. IC₅₀ Values, cLogP, PSA and MW for Compounds 16, 27 and 30

no.	IC ₅₀ μ M (95% confidence interval) ^a			cLogP ^b	PSA ^c	MW
	SIRT1	SIRT2	SIRT3			
16	0.24 (0.22–0.25)	1.80 (1.44–2.26)	3.89 (3.47–4.37)	2.61	287.85	568.69
27	0.89 (0.83–0.96)	2.53 (2.37–2.70)	8.35 (7.37–9.46)	3.66	262.74	485.60
30	5.98 (5.25–6.81)	25.8 (22.7–29.3)	29.4 (23.1–37.4)	4.50	257.70	510.65

^aFluor de Lys assay; values are calculated from three independent determinations giving altogether 27 data points. ^bCalculated logarithm of octanol/water partition coefficient, calculated with MOE 2011.10. ^cTotal polar surface area (\AA^2), calculated with MOE 2011.10.³⁴

compound 38, the N-terminal Cbz group of compound 32 was replaced by a phenylethyl group giving decreased SIRT2 and SIRT3 inhibition. However, compound 39 with an ortho-fluoro substituent on the phenyl ring shows improved affinity toward all studied sirtuins compared to compounds 32 and 38. The fluorine provides an H-bond acceptor that may form an additional H-bond to the enzyme backbone (Leu298 in SIRT3), but the GlideScore scoring function does not reward fluorine as a H-bond acceptor. Finally, two compounds with C-terminal benzyl groups were studied (36 and 37). These compounds have an N-terminal phenyl moiety at the end of a long, flexible chain. The length of these N-terminal moieties is similar to that of the Cbz-4-hydroxy-L-prolyl group. The flexibility of the chains of 36 and 37 allows the phenyl groups be buried deep in the lipophilic cavity. This gives excellent SIRT1 inhibition and good SIRT2 and SIRT3 inhibition.

Three compounds with slightly different inhibition profiles, 16, 27 and 30, were chosen for IC₅₀ profile evaluation and cellular studies. Compound 16 was chosen because it is the only compound giving $\geq 90\%$ inhibition of all studied sirtuins. Compound 27 gives excellent SIRT1 and SIRT2 inhibition (97%) but slightly decreased SIRT3 inhibition (82%). Compound 30 has the highest selectivity toward SIRT1 among these three compounds; it shows 88% SIRT1 inhibition but 66% SIRT2 and 63% SIRT3 inhibition. Compounds 16 and 27 fulfill completely the binding hypothesis while compound 30 with its C-terminal tryptamine shows an alternative H-bond. The IC₅₀ values of the three chosen compounds (Table 4, Figure 6) follow nicely the preliminary screening results, showing slightly different inhibition profiles. Also our previous experience with the thioacetylated compounds has indicated that the preliminary screening correlates well with the IC₅₀ values. This may be due to the reaction mechanism and formation of the stable 1'-S-alkylamidate intermediate.

The Effects of Compounds 16, 27, and 30 in Human Cell Lines. To get the first glimpse of the cell penetration of the compounds, they were studied in two different cell-lines that we have previously used for this purpose, ARPE-19 retinal pigment epithelium cells and SH-SY5Y neuroblastoma cells.³² In the literature, ARPE-19 cells have been used to investigate age-related macular degeneration, where SIRT1 is expected to have a therapeutic role³⁵ and in SH-SY5Y cells SIRT1 has been shown to have neuroprotective effects.³⁶ Because SIRT1 is known to deacetylate Lys382 of p53,^{31,37} Western blot analysis was performed in order to detect changes in acetylation level of p53 after etoposide-induced DNA damage. Each of the compounds showed increased p53 acetylation in ARPE cells, while the effect in SH-SY5Y cells was not as evident (Figure 7A). The low levels of lactate dehydrogenase (LDH) leakage from the treated cells indicated that the tested compounds were not toxic to the cells at the used concentration (Figure 7B).

As sirtuin inhibition has been suggested as a potential therapy for breast and lung cancers,^{16,17,38} the effects of SIRT inhibitors 16, 27, and 30 on the proliferation of two tumor cell lines, A549 lung carcinoma and MCF-7 breast carcinoma, were measured with sulforhodamine B assay. The cell growth of both A549 and MCF-7 was inhibited with $\geq 50 \mu\text{M}$ of 27 and 30 (Figure 8). The other tested SIRT inhibitor 16 did not show any substantial inhibitory effect on A549 or MCF-7 cell growth with concentrations up to 200 μM (data not shown).

In order to understand the different inhibitory behavior of the three tested inhibitors on cell proliferation, the cellular p53 and α -tubulin acetylation levels in the MCF-7 cells were examined, and physicochemical parameters for the inhibitors were calculated (Table 4). The study showed that all three compounds were able to increase the acetylation level of p53, but compound 16 was less effective than 27 and 30 (Figure 9A). Instead, no significant effect was observed on the α -tubulin acetylation status by any of the compounds at 50 μM .

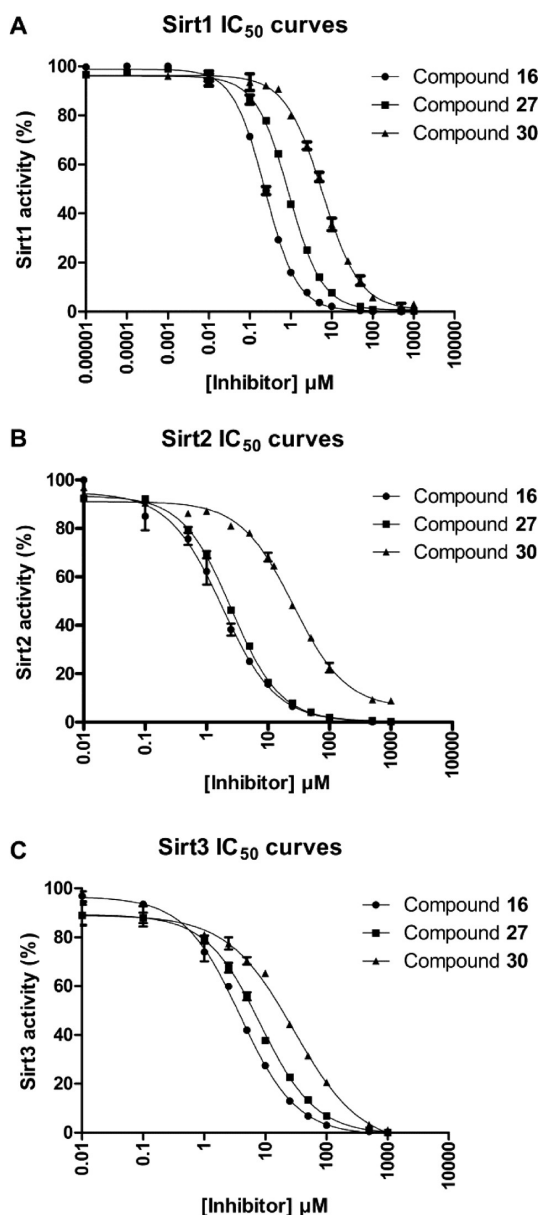


Figure 6. IC_{50} curves of compounds 16, 27 and 30 for (A) SIRT1, (B) SIRT2 and (C) SIRT3.

concentration. Despite being a potent SIRT1–3 inhibitor, compound 16 did not inhibit MCF-7 or A549 cell proliferation. This could be explained by cell-type specific differences in membrane permeability, together with different physicochemical properties of the compounds (Table 4). As these compounds are rather large, it can be speculated that compound 16 with the lowest cLogP and the highest polar surface area and molecular weight may have difficulties in cell permeation. The compounds did not show any toxic effect when tested with LDH assay (Figure 9B).

Propidium iodide staining and flow cytometric DNA content analysis of MCF-7 and A549 cells treated with 27 and 30 was performed in order to detect the effect of these compounds on cell cycle progression. Cell cycle analysis revealed that both 27 and 30 arrested cancer cells in the G_1 phase, with >50% reduction in DNA synthesis (S phase population), and no cell death was observed (Figure 10).

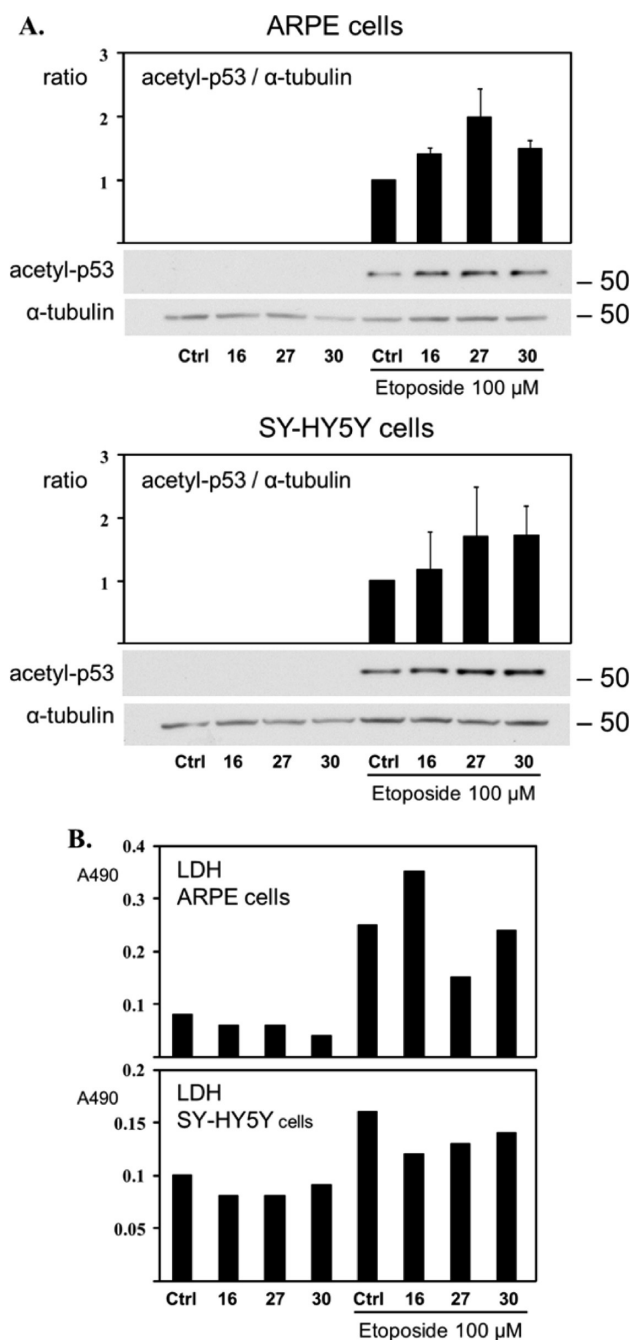


Figure 7. Inhibition of SIRT1 activity increases p53 acetylation after DNA damage. (A) Effect of 20 μM compounds 16, 27, and 30 on p53 acetylation after 100 μM etoposide (eto) treatment for 5 h in ARPE-19 and SH-SY5Y cell lines. The results are shown as mean \pm SEM of two independent experiments. The representative Western blots are shown below. (B) Effect of compounds 16, 27 and 30 on LDH leakage from ARPE-19 and SH-SY5Y cells.

CONCLUSIONS

A library of 30 novel compounds around thioacetylated lysine scaffold was synthesized. The C-terminal 2-oxo-2-phenylethyl and benzyl moieties were found to be fragments that give excellent SIRT1 inhibitions (2, 12–18 and 26, 35–37). The N-terminal Cbz-4-hydroxy-L-prolyl or a long flexible chain attached to a phenyl group (16, 23, 35 and 14, 36, 37) also gave a positive contribution to the binding hypothesis, hinting

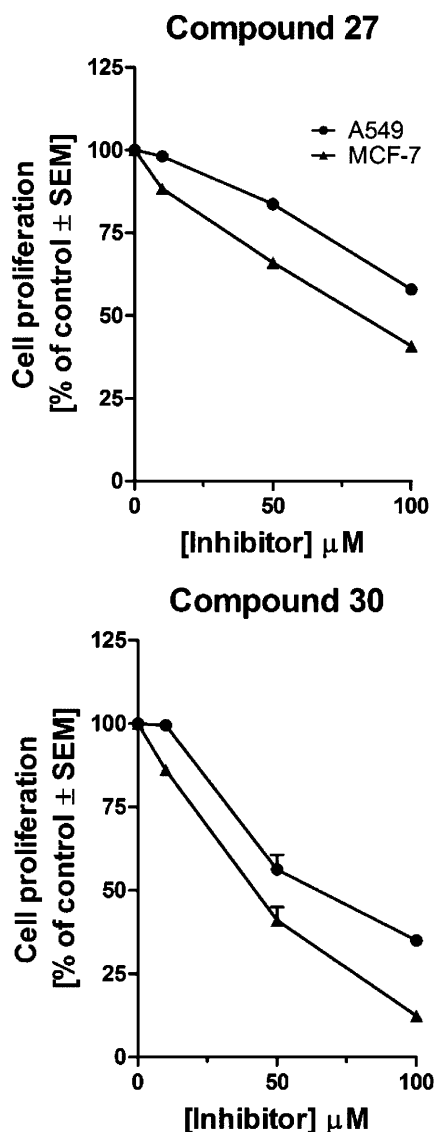


Figure 8. Effects of SIRT inhibitors on A549 and MCF-7 cell proliferation. The cells were treated with 0 to 100 μM of 27 (left) or 30 (right). Cell proliferation was determined by sulforhodamine B assay. The results are shown as mean \pm SEM of two to three independent experiments.

that the H-bond with Gly295 and groups that can be buried deep in the lipophilic cavity can improve inhibition potency.

Three compounds, 16, 27 and 30, with slightly different inhibition profiles were chosen for more detailed studies. Their effect on tumor cell proliferation was studied in A549 lung carcinoma and MCF-7 breast carcinoma cell lines. Interestingly, the in vitro inhibition potency did not correlate with the cellular effect; the most potent compound, 16, did not show any antiproliferative effect, while the two other compounds inhibited cell growth at $\geq 50 \mu\text{M}$ concentration. The difference may arise from different cell permeation of the compounds. Due to the observed induction of p53 acetylation in ARPE-19 and MCF-7 cells, SIRT1 is likely to be one of the cellular targets of compounds 27 and 30.

Compounds 27 and 30 were shown to be cell permeable and nontoxic sirtuin inhibitors. They both inhibited cell growth by the arrest at the G_1 phase in two tumor cell lines, although the effect of compound 30 was more pronounced. These two

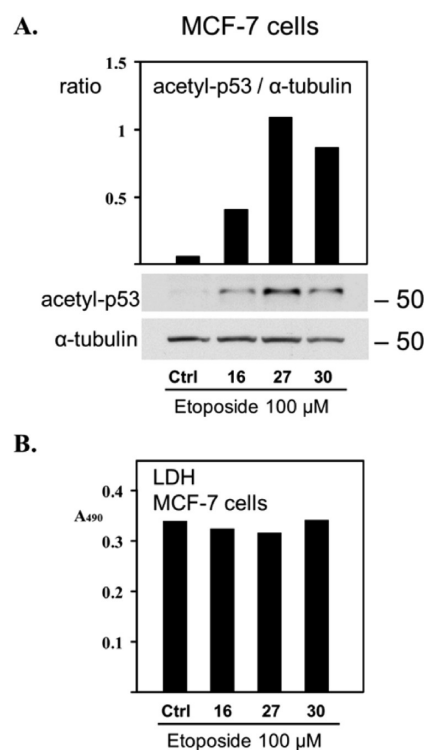


Figure 9. Inhibition of SIRT1 activity increases p53 acetylation after DNA damage in MCF-7 cells. (A) Effect of 50 μM compounds 16, 27, and 30 on p53 acetylation in MCF-7 cells after 100 μM etoposide (eto) treatment for 5 h. The test was performed once for each compound. (B) Effect of compounds 16, 27, and 30 on LDH leakage from MCF-7 cells.

inhibitors are our new lead compounds that will be taken to further studies.

EXPERIMENTAL SECTION

Chemistry. Chemical reagents and solvents used in this study were of commercial high-purity quality. Organic solutions were dried over anhydrous sodium sulfate. Pyridine and dimethylformamide (DMF) were dried over molecular sieves. Compounds 1, 24 were prepared using the same amounts and following the procedure reported by Huhtiniemi and co-workers.^{25,32} Yields of all reactions refer to the purified products. NMR spectra were acquired on a Bruker Avance 500 AV (Bruker Biospin, Switzerland) spectrometer operating at 500.1 MHz for ^1H and 125.8 MHz for ^{13}C . Chemical shift values are reported as δ (ppm) relatively to TMS (tetramethylsilane) as an internal reference; coupling constants are given in hertz. Positive ion mass spectra were recorded with a quadrupole ion trap mass spectrometer (Finnigan MAT, San Jose, CA) equipped with an electrospray ionization source (ESI-MS). The purity of the compounds was determined by elemental analysis obtained by a Thermo Quest CE Instruments EA 1110 CHNS-O elemental analyzer, and the analytical results are within $\pm 0.40\%$ of the theoretical values (see Supporting Information). Purity of tested compounds was $\geq 95\%$. The purity of compounds 27 and 28 was also determined by HPLC (Agilent 1100 series) on a C-18 column (Zorbax Eclipse XDB-C18, 4.6 mm \times 50 mm, 1.8 μm) using 45% acetate buffer (20 mM, pH 5) and 55% MeOH as eluent, flow rate 1 mL/min, column temperature 50 $^\circ\text{C}$ and detection at 265 nm.

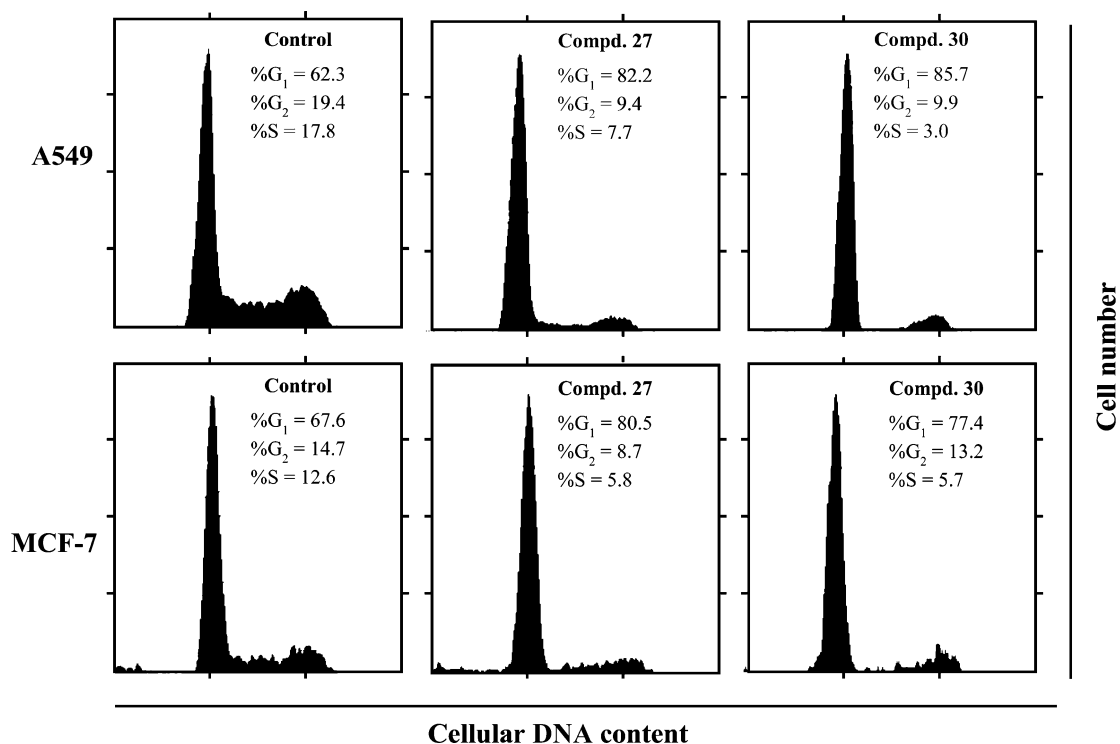


Figure 10. Effects of SIRT inhibitors on A549 and MCF-7 cell cycles. The cells were subjected to control treatment (0.5% DMSO) or treatment with 100 μ M of 27 or 30 for 18 h. Flow cytometric analysis of DNA content was done after propidium iodide staining. Percentage of cells in each phase of the cell cycle (G₁, G₂, and S) is indicated. Representative data from at least two independent experiments are shown.

General Procedure for the Coupling Reactions of the End Products 2, 6, 12–21, 23, 25–40: (2S)-2-tert-Butyl 6-Ethanethioamido-1-oxo-1-(2-oxo-2-phenylethylamino)-hexan-2-ylcarbamate (2). To a solution of the acid 1 (1.17 g, 1.0 equiv, 3.84 mmol) in DMF (17.0 mL) under argon flow were added TBTU (1.36 g, 1.1 equiv, 4.2 mmol), pyridine (17.0 mL) and maintained under stirring for 10 min at rt. After this time 2-aminoacetophenone hydrochloride (0.66 g, 3.84 mmol) was added and the solution mixed 2 h 30 min at rt under Argon flow. Solvents were evaporated and the obtained oil was dissolved in EtOAc (180 mL), washed with HCl 0.5M, brine (two times), saturated NaHCO₃ and finally dried with Na₂SO₄ and evaporated under vacuo. The crude product obtained was purified by column chromatography using silica Kieselgel for flash and EtOAc: MeOH (9.5: 0.5 v/v) as eluent phase to give the pure product as a sticky solid (1.34 g, 3.17 mmol, 83%). ¹H NMR (DMSO-*d*₆): δ = 9.95 (s br, 1H), 8.13 (t, *J* = 5.36 Hz, 1H), 7.99 (d, *J* = 7.57 Hz, 2H), 7.67 (t, *J* = 7.57 Hz, 1H), 7.54 (t, *J* = 7.57 Hz, 2H), 6.90 (d, *J* = 8.20 Hz, 1H), 4.70–4.54 (m, 2H), 4.01–3.97 (m, 1H), 3.50–3.39 (m, 2H), 2.39 (s, 3H), 1.71–1.49 (m, 4H), 1.39–1.30 (m, 11H). ¹³C NMR (CDCl₃): δ = 201.06, 194.12, 172.33, 155.96, 134.43, 134.39, 129.13, 128.07, 54.11, 46.42, 46.12, 34.22, 32.67, 29.82, 28.46, 27.16, 22.88. ESI-MS (*m/z*): 422.0 [M + H]⁺, 444.20 [M + Na]⁺. Anal. (C₂₁H₃₁N₃O₄S) C, H, N.

(2S)-2-tert-Butyl 6-ethanethioamido-1-oxo-1-[2-(pyridin-3-yl)ethylamino]hexan-2-ylcarbamate (6): ¹H NMR (DMSO-*d*₆): δ = 9.93 (s br, 1H), 8.42 (m, 2H), 7.87 (t, *J* = 5.36 Hz, 1H), 7.62 (dt, *J* = 1.60, 7.57 Hz, 1H), 7.30 (dd, *J* = 4.73, 7.57 Hz, 1H), 6.75 (d, *J* = 8.20 Hz, 1H), 3.84–3.79 (m, 1H), 3.44–3.24 (m, 4H), 2.74–2.71 (m, 2H), 2.37 (s, 3H), 1.52–1.34 (m, 13H), 1.25–1.16 (m, 2H). ¹³C NMR (DMSO-*d*₆): δ = 198.77, 172.10, 155.29, 149.59, 147.09, 136.66, 135.07, 123.47,

77.98, 54.25, 45.28, 32.81, 32.07, 31.74, 28.21, 26.93, 23.04, (–NH–CH₂–CH₂–pyr under DMSO-*d*₆). ESI-MS (*m/z*): 409.15 [M + H]⁺. Anal. (C₂₀H₃₂N₄O₃S·0.03DMF·0.03hexane) C, H, N.

(2S)-2-(3-Phenylpropanoylamino)-6-ethanethioylamino-N-(2-oxo-2-phenylethyl)hexanamide (12): ¹H NMR (DMSO-*d*₆): δ = 9.95 (s br, 1H), 8.24 (t, *J* = 5.36 Hz, 1H), 8.03 (d, *J* = 8.20 Hz, 1H), 7.99 (d, *J* = 7.57 Hz, 2H), 7.67 (t, *J* = 7.57 Hz, 1H), 7.54 (t, *J* = 7.57 Hz, 2H), 7.28–7.15 (–Ar, 5H), 4.65–4.55 (m, 2H), 4.37–4.32 (m, 1H), 3.46–3.38 (m, 2H), 2.84–2.79 (m, 2H), 2.47–2.43 (m, 2H), 2.38 (s, 3H), 1.70–1.62 (m, 1H), 1.55–1.47 (m, 3H), 1.29–1.22 (m, 2H). ¹³C NMR (DMSO-*d*₆): δ = 198.74, 195.13, 172.11, 171.35, 141.27, 134.95, 133.50, 128.77, 128.20, 128.17, 127.79, 125.80, 52.16, 45.83, 45.33, 36.72, 32.78, 31.83, 31.04, 26.90, 22.82. ESI-MS (*m/z*): 454.14 [M + H]⁺. Anal. (C₂₅H₃₁N₃O₃S) C, H, N.

(2S)-2-(4-Phenylbutyrylamino)-6-ethanethioylamino-N-(2-oxo-2-phenylethyl)hexanamide (13): ¹H NMR (DMSO-*d*₆): δ = 9.93 (s br, 1H), 8.21 (t, *J* = 5.36 Hz, 1H), 7.98–7.96 (m, 3H), 7.65 (t, *J* = 7.25 Hz, 1H), 7.54 (t, *J* = 7.25 Hz, 2H), 7.29–7.16 (–Ar, 5H), 4.66–4.54 (m, 2H), 4.37–4.32 (m, 1H), 3.47–3.42 (m, 2H), 2.58–2.52 (m, 2H), 2.37 (s, 3H), 2.18–2.15 (m, 2H), 1.83–1.77 (m, 2H), 1.74–1.67 (m, 1H), 1.60–1.50 (m, 3H), 1.37–1.28 (m, 2H). ¹³C NMR (DMSO-*d*₆): 198.69, 195.10, 172.17, 171.86, 141.82, 134.95, 133.50, 128.76, 128.31, 128.23, 127.79, 125.69, 52.19, 45.85, 45.32, 34.66, 34.66, 32.78, 31.72, 27.08, 26.89, 22.97. ESI-MS (*m/z*): 468.20 [M + H]⁺. Anal. (C₂₆H₃₃N₃O₃S) C, H, N.

(2S)-2-(6-Phenylhexanoylamino)-6-ethanethioylamino-N-(2-oxo-2-phenylethyl)hexanamide (14): ¹H NMR (DMSO-*d*₆): δ = 9.93 (s br, 1H), 8.20 (t, *J* = 5.67 Hz, 1H), 7.97 (d, *J* = 7.25 Hz, 2H), 7.92 (d, *J* = 8.20 Hz, 1H), 7.66 (t, *J* = 7.25 Hz, 1H), 7.54 (t, *J* = 7.25 Hz, 2H), 7.27–7.14 (–Ar, 5H),

4.65–4.54 (m, 2H), 4.36–4.31 (m, 1H), 3.46–3.42 (m, 2H), 2.57–2.54 (m, 2H), 2.38 (s, 3H), 2.18–2.10 (m, 2H), 1.73–1.66 (m, 1H), 1.59–1.49 (m, 7H), 1.36–1.24 (m, 4H). ^{13}C NMR (DMSO- d_6): 198.75, 195.13, 172.21, 172.15, 142.25, 134.95, 133.51, 128.77, 128.22, 128.17, 127.79, 125.55, 52.10, 45.84, 45.33, 35.08, 35.05, 32.78, 31.77, 30.75, 28.27, 26.89, 25.07, 22.92. ESI-MS (m/z): 496.22 $[\text{M} + \text{H}]^+$. Anal. ($\text{C}_{28}\text{H}_{37}\text{N}_3\text{O}_3\text{S}$) C, H, N.

(2S)-2-[3-(Pyridine-3-yl)propanoylamino]-6-ethanethiylamino-N-(2-oxo-2-phenylethyl) hexanamide (15): ^1H NMR (DMSO- d_6): δ = 9.97 (s br, 1H), 8.43 (s, 1H), 8.38 (d, J = 4.41 Hz, 1H), 8.27 (t, J = 5.36 Hz, 1H), 8.06 (d, J = 8.20 Hz, 1H), 7.99 (d, J = 7.57 Hz, 2H), 7.67 (t, J = 7.57 Hz, 1H), 7.62 (d, J = 7.47 Hz, 1H), 7.54 (t, J = 7.57 Hz, 2H), 7.29 (dd, J = 4.41, 7.47 Hz, 1H), 4.65–4.55 (m, 2H), 4.36–4.32 (m, 1H), 3.44–3.38 (m, 2H), 2.85–2.82 (m, 2H), 2.55–2.42 (m, 2H), 2.38 (s, 3H), 1.69–1.62 (m, 1H), 1.55–1.44 (m, 3H), 1.27–1.18 (m, 2H). ^{13}C NMR (DMSO- d_6): δ = 199.21, 195.61, 172.57, 171.48, 150.03, 147.67, 137.09, 136.28, 135.40, 134.03, 129.27, 128.30, 123.81, 52.61, 46.31, 45.81, 36.63, 33.27, 32.37, 28.58, 27.37, 23.29. ESI-MS (m/z): 455.19 $[\text{M} + \text{H}]^+$. Anal. ($\text{C}_{24}\text{H}_{30}\text{N}_4\text{O}_3\text{S} \cdot 0.5 \text{H}_2\text{O}$) C, H, N.

(2S,4R)-N-[(2S)-6-Ethanethiylamino-1-(2-oxo-2-phenylethylamino)-1-oxohexan-2-yl]-4-hydroxypyrrolidine-1-benzoyloxycarbonyl-2-carboxamide (16): ^1H NMR (DMSO- d_6): rotamers A+B δ = 9.91–9.88 (m br, 1H), 8.19–8.13 (m, 2H), 7.99 (t, J = 7.57 Hz, 2H), 7.67 (t, J = 7.57 Hz, 1H), 7.54 (t, J = 7.57 Hz, 2H), 7.37–7.28 (–Ar, 5H), 5.10–4.97 (m, 3H), 4.57–4.53 (m, 2H), 4.43–4.41 (m, 0.5H), 4.35–4.26 (m, 2.5H), 3.52–3.44 (m, 2H), 3.39–3.35 (m, 2H), 2.38 (s, 1.5H), 2.37 (s, 1.5H) 2.14–2.05 (m, 1H), 1.90–1.86 (m, 1H), 1.78–1.72 (m, 0.5H), 1.65–1.52 (m, 1.5H), 1.48–1.34 (m, 2.5H), 1.29–1.19 (m, 1.5H). ^{13}C NMR (DMSO- d_6): rotamers A+(B) δ = 198.72, 195.11, 172.01 (171.90), 171.85 (171.71), 154.29 (154.01), 136.90, 134.92, 133.54, 128.78, 128.37 (128.17), 127.80, 127.46, 126.89, 68.48 (67.77), 65.93 (65.79), 58.80 (58.09), 55.34 (54.87), 52.39 (52.24), 45.85, 45.39 (45.29), 38.51, 32.77, 31.77 (31.57), 26.90 (26.82), 22.78. ESI-MS (m/z): 569.15 $[\text{M} + \text{H}]^+$. Anal. ($\text{C}_{29}\text{H}_{36}\text{N}_4\text{O}_6\text{S}$) C, H, N.

(2S)-N-[(2S)-6-Ethanethiylamino-1-(2-oxo-2-phenylethylamino)-1-oxohexan-2-yl]-pyrrolidine-1-tert-butoxycarbonyl-2-carboxamide (17): ^1H NMR (DMSO- d_6): rotamers A+B δ = 9.91 (s br, 1H), 8.27 (t, J = 5.36 Hz, 0.6H), 8.15 (t, J = 5.36 Hz, 0.4H), 7.98–7.92 (m, 3H), 7.66 (t, J = 7.25 Hz, 1H), 7.54 (t, J = 7.25 Hz, 2H), 4.69–4.55 (m, 2H), 4.39–4.32 (m, 1H), 4.17–4.15 (m, 1H), 3.47–3.37 (m, 3H), 3.28–3.25 (m, 1H), 2.38 (s, 3H), 2.14–2.00 (m, 1H), 1.86–1.67 (m, 4H), 1.62–1.52 (m, 3H), 1.41–1.30 (m, 11H). ^{13}C NMR (DMSO- d_6): rotamers A+(B) δ = 198.77, 195.11 (195.03), 172.33, 171.97 (171.93), 153.76 (153.26), 134.92, 133.53, 128.78, 127.80, 78.64 (78.29), 59.28, 52.15, 46.74 (46.49), 45.85, 45.30, 32.77, 32.05 (31.80), 31.00 (29.58), 28.11 (28.00), 26.91, 23.98 (23.02), 22.85 (22.75). ESI-MS (m/z): 519.03 $[\text{M} + \text{H}]^+$. Anal. ($\text{C}_{26}\text{H}_{38}\text{N}_4\text{O}_5\text{S}$) C, H, N.

(S)-2-(2-((2S,5S)-5-Benzyl-3,6-dioxopiperazin-2-yl)-acetamido)-6-ethanethioamido-N-(2-oxo-2-phenylethyl)hexanamide (18): ^1H NMR (DMSO- d_6): δ = 9.94 (s br, 1H), 8.28 (t, J = 5.67 Hz, 1H), 8.20 (s, 1H), 8.02 (d, J = 7.88 Hz, 1H), 7.97 (d, J = 7.57 Hz, 2H), 7.69–7.64 (m, 2H), 7.53 (t, J = 7.57 Hz, 2H), 7.29–7.19 (–Ar, 5H), 4.63–4.50 (m, 2H), 4.25–4.21 (m, 2H), 4.13–4.10 (m, 1H), 3.49–3.45 (m, 2H), 3.10 (m, 1H), 2.94 (m, 1H), 2.38–2.35 (m, 4H),

1.77–1.71 (m, 1H), 1.63–1.52 (m, 4H), 1.37–1.29 (m, 2H). ^{13}C NMR (DMSO- d_6): δ = 198.91, 195.09, 172.02, 169.43, 167.19, 166.51, 136.47, 134.81, 133.39, 130.21, 128.71, 128.01, 127.63, 126.75, 54.87, 52.73, 51.50, 45.72, 45.52, 38.57, 37.67, 32.97, 31.41, 26.75, 22.81. ESI-MS (m/z): 566.14 $[\text{M} + \text{H}]^+$, 588.23 $[\text{M} + \text{Na}]^+$. Anal. ($\text{C}_{29}\text{H}_{35}\text{N}_5\text{O}_5\text{S}$) C, H, N.

(2S)-6-(Ethanethiylamino)-N-phenyl-2-[3-(pyridin-3-yl)propanoylamino]hexanamide (19): ^1H NMR (DMSO- d_6): δ = 10.04 (s, 1H), 9.97 (s br, 1H), 8.44 (s, 1H), 8.38 (d, J = 4.88 Hz, 1H), 8.17 (d, J = 7.93 Hz, 1H), 7.63–7.58 (m, 3H), 7.32–7.27 (m, 3H), 7.05 (m, 1H), 4.40–4.36 (m, 1H), 3.44–3.41 (m, 2H), 2.85–2.82 (m, 2H), 2.54–2.46 (m, 2H), 2.36 (s, 3H), 1.69–1.62 (m, 1H), 1.57–1.48 (m, 3H), 1.32–1.18 (m, 2H). ^{13}C NMR (DMSO- d_6): δ = 198.80, 171.19, 170.76, 149.56, 147.18, 138.89, 136.57, 135.77, 128.68, 128.68, 123.29, 119.28, 53.22, 45.24, 36.07, 32.79, 31.81, 28.13, 26.92, 22.96. ESI-MS (m/z): 413.22 $[\text{M} + \text{H}]^+$. Anal. ($\text{C}_{22}\text{H}_{28}\text{N}_4\text{O}_2\text{S}$) C, H, N.

(2S)-6-(Ethanethiylamino)-N-phenyl-2-[(dimethylamino)acetylamin]-hexanamide (20): ^1H NMR (DMSO- d_6): δ = 10.08 (s, 1H), 9.94 (s br, 1H) 7.82 (d, J = 8.20 Hz, 1H), 7.58 (d, J = 7.88 Hz, 2H), 7.30 (t, J = 7.88 Hz, 2H), 7.05 (t, J = 7.88 Hz, 1H), 4.50–4.45 (m, 1H), 3.46–3.43 (m, 2H), 2.95 (d, J = 15.26 Hz, 1H) 2.92 (d, J = 15.26 Hz, 1H), 2.35 (s, 3H), 2.24 (s, 6H), 1.78–1.52 (m, 4H), 1.39–1.23 (m, 2H). ^{13}C NMR (DMSO- d_6): δ = 199.28, 170.93, 169.90, 139.22, 129.20, 123.91, 119.77, 62.94, 53.12, 45.89, 45.65, 33.24, 32.62, 27.38, 23.37. ESI-MS (m/z): 365.19 $[\text{M} + \text{H}]^+$. Anal. ($\text{C}_{18}\text{H}_{28}\text{N}_4\text{O}_2\text{S}$) C, H, N.

(2S)-N-[(2S)-6-Ethanethiylamino-1-phenylamino-1-oxohexan-2-yl]-pyrrolidine-1-tert-butoxycarbonyl-2-carboxamide (21): ^1H NMR (DMSO- d_6): rotamers A+B δ = 10.06 (s, 0.6H), 9.93 (s br, 1H), 9.84 (s, 0.4H), 8.04 (d, J = 7.88 Hz, 1H), 7.59 (d, J = 7.57 Hz, 2H), 7.30 (t, J = 7.57 Hz, 2H), 7.04 (t, J = 7.57 Hz, 1H), 4.43–4.33 (m, 1H), 4.19–4.15 (m, 1H), 3.45–3.36 (m, 3H), 3.29–3.24 (m, 1H), 2.36 (s, 3H), 2.15–2.04 (m, 1H), 1.83–1.52 (m, 7H), 1.45–1.23 (m, 11H). ^{13}C NMR (DMSO- d_6): rotamers A+(B) δ = 198.79, 172.55 (172.18), 170.58, 153.88 (153.29), 138.89 (138.81), 128.67, 123.27, 119.21 (119.14), 78.76 (78.34), 59.36 (59.31), 53.21, 46.72 (46.50), 45.22 (45.16), 32.75, 31.83 (31.49), 30.99 (29.77), 28.11 (27.98), 26.90, 23.91, 23.05 (23.02). ESI-MS (m/z): 477.03 $[\text{M} + \text{H}]^+$, 499.19 $[\text{M} + \text{Na}]^+$. Anal. ($\text{C}_{24}\text{H}_{36}\text{N}_4\text{O}_4\text{S}$) C, H, N.

(2S)-N-[(2S)-6-Ethanethiylamino-1-(phenylamino)-1-oxohexan-2-yl]-pyrrolidine-2-carboxamide Hydrochloride (22). To a solution of **21** (0.10 g, 0.21 mmol) in 2-propanol (3.6 mL) was added 1,2-ethanedithiol (0.018 mL, 0.21 mmol), and after 1 min under stirring at rt was added HCl 12 N (0.11 mL, 1.32 mmol). Then the solution was heated to 60 °C; after 20 and 40 min a portion of HCl 12 N (each portion 0.11 mL) was added; when the total amount of HCl in the reaction flask was 3.96 mmol, the solution was maintained for 60 min at 60 °C under stirring. After this time, 2-propanol was evaporated under reduced pressure, and the yellow oil was washed with petroleum ether (4 \times 10 mL) and CH_2Cl_2 /petroleum ether (1:1) (4 \times 4 mL), providing the product as white solid (0.077 g, 0.18 mmol, 85%). ^1H NMR (DMSO- d_6): δ = 10.23 (s, 1H), 10.11 (s br, 1H), 9.72 (s br, 1H), 8.85 (d, J = 7.57 Hz, 1H), 8.49 (s br, 1H), 7.61 (d, J = 7.25 Hz, 2H), 7.30 (t, J = 7.25 Hz, 2H), 7.05 (t, J = 7.25 Hz, 1H), 4.46–4.42 (m, 1H), 4.28–4.23 (m, 1H), 3.49–3.45 (m, 2H), 3.24–3.16 (m, 2H), 2.38–2.33 (m, 4H), 1.89–1.55 (m, 7H), 1.48–1.31 (m,

2H). ^{13}C NMR (DMSO- d_6): δ = 198.77, 170.01, 168.22, 138.86, 128.69, 123.36, 119.21, 58.62, 53.95, 45.58, 45.03, 32.74, 31.58, 29.62, 26.81, 23.46, 23.07. ESI-MS (m/z): 377.20 $[\text{M} + \text{H}]^+$. Anal. ($\text{C}_{19}\text{H}_{29}\text{ClN}_4\text{O}_2\text{S} \cdot 0.3\text{H}_2\text{O}$) C, H, N.

(2S,4R)-N-[(2S)-6-Ethanethioylamino-1-phenylamino-1-oxohexan-2-yl]-4-hydroxypyrrolidine-1-benzoyloxycarbonyl-2-carboxamide (23): ^1H NMR (DMSO- d_6): rotamers A+B δ = 10.04 (s, 0.55H), 9.93–9.90 (m br, 1H), 9.82 (s, 0.45H), 8.26 (m, 1H), 7.63–7.59 (m, 2H), 7.37–7.30 (m, 7H), 7.08–7.03 (m, 1H), 5.13–4.97 (m, 3H), 4.44–4.41 (m, 0.5H), 4.38–4.34 (m, 1.5H), 4.28–4.23 (m, 1H), 3.53–3.47 (m, 2H), 3.39–3.35 (m, 2H), 2.36 (s, 1.45H), 2.35 (s, 1.55H) 2.14–2.07 (m, 1H), 1.90–1.84 (m, 1H), 1.79–1.73 (m, 0.5H), 1.67–1.20 (m, 5.5H). ^{13}C NMR (DMSO- d_6): rotamers A+(B) δ = 198.77, 172.14 (171.83), 170.54, 154.43 (154.01), 138.88 (138.83), 136.86 (136.82), 128.68, 128.38 (128.16), 127.78 (127.49), 127.42 (126.94), 123.32 (123.28), 119.19 (119.11), 68.40 (67.60), 65.92 (65.87), 58.90 (57.90), 55.40 (54.80), 53.38 (53.30), 45.26 (45.20), 38.63, 32.75, 31.80 (31.38), 26.92 (26.72), 22.85 (22.80). ESI-MS (m/z): 527.11 $[\text{M} + \text{H}]^+$. Anal. ($\text{C}_{27}\text{H}_{34}\text{N}_4\text{O}_5\text{S}$) C, H, N.

(2S)-2-Benzyl 6-ethanethioamido-1-oxo-1-(2-phenylethylamino)hexan-2-ylcarbamate (25): ^1H NMR (CDCl_3): δ = 7.77 (s br, 1H), 7.39–7.29 (m, 7H), 7.25–7.22 (m, 1H), 7.18 (m, 2H), 6.12 (s br, 1H), 5.45 (d, J = 7.57 Hz, 1H), 5.09 (s, 2H), 4.12–4.07 (m, 1H), 3.65–3.46 (m, 4H), 2.82–2.80 (m, 2H), 2.54 (s, 3H), 1.81–1.74 (m, 1H), 1.68–1.59 (m, 3H), 1.40–1.33 (m, 2H). ^{13}C NMR (DMSO- d_6): δ = 198.75, 171.57, 155.81, 139.31, 136.98, 128.54, 128.21, 128.15, 127.64, 127.55, 125.94, 65.31, 54.63, 45.19, 40.02, 34.99, 32.74, 31.65, 26.83, 22.93. ESI-MS (m/z): 442.20 $[\text{M} + \text{H}]^+$. Anal. ($\text{C}_{24}\text{H}_{31}\text{N}_3\text{O}_3\text{S}$) C, H, N.

(2S)-2-Benzyl 6-ethanethioamido-1-oxo-1-(benzylamino)hexan-2-ylcarbamate (26): ^1H NMR (CDCl_3): δ = 7.69 (s br, 1H), 7.38–7.29 (m, 8H), 7.26–7.24 (m, 2H), 6.41 (s br, 1H), 5.45 (d, J = 7.57 Hz, 1H), 5.09 (s, 2H), 4.48–4.40 (m, 2H), 4.23–4.19 (m, 1H), 3.68–3.60 (m, 2H), 2.53 (s, 3H), 1.91–1.86 (m, 1H), 1.75–1.68 (m, 3H), 1.45–1.39 (m, 2H). ^{13}C NMR (DMSO- d_6): δ = 198.74, 171.80, 155.90, 139.28, 136.97, 128.21, 128.11, 127.64, 127.55, 126.98, 126.58, 65.32, 54.67, 45.18, 41.97, 32.73, 31.56, 26.79, 23.01. ESI-MS (m/z): 428.18 $[\text{M} + \text{H}]^+$, 450.19 $[\text{M} + \text{Na}]^+$. Anal. ($\text{C}_{23}\text{H}_{29}\text{N}_3\text{O}_3\text{S}$) C, H, N.

(2S)-2-Benzyl 6-ethanethioamido-1-oxo-1-[2-oxo-2-(4-methoxyphenyl)ethylamino]hexan-2-ylcarbamate (27): ^1H NMR (DMSO- d_6): δ = 9.93 (s br, 1H), 8.17 (t, J = 5.36 Hz, 1H), 7.97 (d, J = 8.83 Hz, 2H), 7.45 (d, J = 8.20 Hz, 1H), 7.37–7.30 (m, 5H), 7.05 (d, J = 8.83 Hz, 2H), 5.06–5.01 (m, 2H), 4.64–4.49 (m, 2H), 4.09–4.05 (m, 1H), 3.84 (s, 3H), 3.48–3.40 (m, 2H), 2.37 (s, 3H), 1.74–1.67 (m, 1H), 1.60–1.50 (m, 3H), 1.41–1.30 (m, 2H). ^{13}C NMR (DMSO- d_6): δ = 198.75, 193.35, 172.26, 163.34, 155.96, 137.03, 130.12, 128.31, 127.81, 127.78, 127.64, 113.98, 65.37, 55.54, 54.58, 45.47, 45.30, 32.80, 31.71, 26.88, 23.05. ESI-MS (m/z): 486.14 $[\text{M} + \text{H}]^+$. HPLC: Rt. 2.64 min, area percent 98.87% 265 nm. Anal. ($\text{C}_{25}\text{H}_{31}\text{N}_3\text{O}_5\text{S} \cdot 0.02\text{hexane}$) C, H, N.

(2S)-2-Benzyl 6-ethanethioamido-1-oxo-1-(2-hydroxy-2-phenylethylamino)hexan-2-ylcarbamate (28): ^1H NMR (DMSO- d_6): diastereoisomer A+B δ = 9.93 (s br, 1H), 7.87–7.83 (m, 1H), 7.40–7.23 (m, 11H), 5.46–5.44 (m, 1H), 5.06–5.00 (m, 2H), 4.63–4.58 (m, 1H), 3.99–3.93 (m, 1H), 3.47–3.39 (m, 2H), 3.36–3.31 (m, 0.4H), 3.26–3.24 (m, 1H), 3.16–3.11 (m, 0.6H), 2.38 (s, 3H), 1.58–1.43 (m, 4H),

1.32–1.18 (m, 2H). ^{13}C NMR (CDCl_3): diastereoisomer A + (B) δ = 200.89 (200.86), 172.75, 156.49, 141.32, 135.92, 128.57, 128.57, 128.31, 128.00, 127.96, 125.75, 73.08 (72.99), 67.19, 54.63, 47.16, 45.79, 33.87, 32.22, 27.04 (27.00). ESI-MS (m/z): 458.14 $[\text{M} + \text{H}]^+$ HPLC: Rt. 1.92 min, area percent 98.91%, 265 nm. Anal. ($\text{C}_{24}\text{H}_{31}\text{N}_3\text{O}_4\text{S} \cdot 0.1\text{hexane} \cdot 0.01\text{EtOAc}$) C, H, N.

(2S)-2-Benzyl 6-ethanethioamido-1-oxo-1-[2-(1H-indol-3-yl)ethylamino]hexan-2-ylcarbamate (29): ^1H NMR (DMSO- d_6): δ = 10.79 (s, 1H), 9.92 (s br, 1H), 7.97 (t, J = 5.67 Hz, 1H), 7.54 (d, J = 7.88 Hz, 1H), 7.37–7.32 (m, 7H), 7.13 (s, 1H), 7.05 (t, J = 7.57 Hz, 1H), 6.97 (t, J = 7.57 Hz, 1H), 5.06–4.99 (m, 2H), 3.95–3.91 (m, 1H), 3.45–3.40 (m, 2H), 3.38–3.26 (m, 2H), 2.82–2.79 (m, 2H), 2.36 (s, 3H), 1.64–1.46 (m, 4H), 1.35–1.22 (m, 2H). ^{13}C NMR (DMSO- d_6): δ = 198.75, 171.65, 155.93, 137.05, 136.21, 128.30, 127.75, 127.67, 127.16, 122.64, 120.87, 118.22, 118.18, 111.68, 111.32, 65.36, 54.69, 45.25, 39.47, 32.79, 31.70, 26.89, 25.13, 23.09. ESI-MS (m/z): 481.17 $[\text{M} + \text{H}]^+$, 503.23 $[\text{M} + \text{Na}]^+$. Anal. ($\text{C}_{26}\text{H}_{32}\text{N}_4\text{O}_3\text{S}$) C, H, N.

(2S)-2-Benzyl 6-ethanethioamido-1-oxo-1-[2-(5-methoxy-1H-indol-3-yl)ethylamino]hexan-2-ylcarbamate (30): ^1H NMR (DMSO- d_6): δ = 10.63 (s, 1H), 9.93 (s br, 1H), 7.97 (t, J = 5.36 Hz, 1H), 7.37–7.22 (m, 7H), 7.10 (s, 1H), 7.03 (s, 1H), 6.71 (d, J = 8.83 Hz, 1H), 5.07–5.00 (m, 2H), 3.97–3.90 (m, 1H), 3.76 (s, 3H), 3.46–3.29 (m, 4H), 2.79 (t, J = 7.25 Hz, 2H), 2.37 (s, 3H), 1.64–1.49 (m, 4H), 1.32–1.24 (m, 2H). ^{13}C NMR (DMSO- d_6): δ = 198.75, 171.67, 155.95, 152.96, 137.06, 131.36, 128.32, 127.76, 127.69, 127.47, 123.32, 111.97, 111.43, 111.02, 100.11, 65.37, 55.34, 54.72, 45.26, 39.34, 32.80, 31.72, 26.91, 25.18, 23.12. ESI-MS (m/z): 511.19 $[\text{M} + \text{H}]^+$. Anal. ($\text{C}_{27}\text{H}_{34}\text{N}_4\text{O}_4\text{S}$) C, H, N.

(2S)-2-Benzyl 6-ethanethioamido-1-oxo-1-[2-(5-benzoyloxy-1H-indol-3-yl)ethylamino]hexan-2-ylcarbamate (31): ^1H NMR (DMSO- d_6): δ = 10.66 (s, 1H), 9.93 (s br, 1H), 7.97 (t, J = 5.36 Hz, 1H), 7.50–7.23 (m, 12H), 7.16 (s, 1H), 7.11 (s, 1H), 6.81 (d, J = 10.40 Hz, 1H), 5.10–5.00 (m, 4H), 3.98–3.93 (m, 1H), 3.48–3.27 (m, 4H), 2.79 (t, J = 7.25 Hz, 2H), 2.37 (s, 3H), 1.61–1.46 (m, 4H), 1.36–1.23 (m, 2H). ^{13}C NMR (DMSO- d_6): δ = 198.76, 171.68, 155.96, 151.98, 137.81, 137.06, 131.56, 128.32, 128.32, 127.76, 127.69, 127.69, 127.59, 127.48, 123.44, 111.97, 111.59, 111.45, 101.83, 69.86, 65.37, 54.72, 45.26, 39.31, 32.80, 31.72, 26.91, 25.17, 23.12. ESI-MS (m/z): 587.22 $[\text{M} + \text{H}]^+$. Anal. ($\text{C}_{33}\text{H}_{38}\text{N}_4\text{O}_4\text{S}$) C, H, N.

(2S)-2-Benzyl 6-ethanethioamido-1-oxo-1-(pyridin-3-ylamino)hexan-2-ylcarbamate (32): ^1H NMR (DMSO- d_6): δ = 10.25 (s, 1H), 9.95 (s br, 1H), 8.76 (d, J = 2.21 Hz, 1H), 8.27 (dd, J = 1.58, 6.31 Hz, 1H), 8.05–8.03 (m, 1H), 7.63 (d, J = 7.57 Hz, 1H), 7.37–7.30 (m, 6H), 5.07–5.01 (m, 2H), 4.17–4.13 (m, 1H), 3.49–3.42 (m, 2H), 2.36 (s, 3H), 1.75–1.50 (m, 4H), 1.46–1.29 (m, 2H). ^{13}C NMR (DMSO- d_6): δ = 198.79, 171.67, 156.12, 144.23, 140.81, 136.95, 135.56, 128.33, 127.80, 127.72, 126.24, 123.63, 65.47, 55.54, 45.16, 32.80, 31.36, 26.91, 23.19. ESI-MS (m/z): 415.19 $[\text{M} + \text{H}]^+$. Anal. ($\text{C}_{21}\text{H}_{26}\text{N}_4\text{O}_3\text{S}$) C, H, N.

(2S)-2-Benzyl 6-ethanethioamido-1-oxo-1-(2-amino-2-oxoethylamino)hexan-2-ylcarbamate (33): ^1H NMR (DMSO- d_6): δ = 9.92 (s br, 1H), 8.10 (t, J = 5.67 Hz, 1H), 7.49 (d, J = 7.57 Hz, 1H), 7.39–7.32 (m, 5H), 7.19 (s, 1H), 7.07 (s, 1H), 5.06–4.99 (m, 2H), 3.99–3.94 (m, 1H), 3.67–3.59 (m, 2H), 3.47–3.41 (m, 2H), 2.37 (s, 3H), 1.70–1.63 (m, 1H), 1.57–1.48 (m, 3H), 1.39–1.23 (m, 2H). ^{13}C NMR (DMSO- d_6): δ = 198.75, 172.04, 170.77, 156.12, 136.91,

128.32, 127.78, 127.69, 65.46, 54.72, 45.26, 41.86, 32.79, 31.27, 26.85, 23.01. ESI-MS (m/z): 395.19 $[M + H]^+$. Anal. ($C_{18}H_{26}N_4O_4S$) C, H, N.

(2S)-2-Benzyl-6-ethanethioamido-1-oxo-1-[(2S)-1-amino-1-oxopropan-2-yl]amino]hexan-2-ylcarbamate (34): 1H NMR (DMSO- d_6): δ = 9.91 (s br, 1H), 7.87 (d, J = 7.25 Hz, 1H), 7.43 (d, J = 8.20 Hz, 1H), 7.38–7.29 (m, 6H), 6.99 (s, 1H), 5.04–4.99 (m, 2H), 4.22–4.16 (m(s), J = 7.25 Hz, 1H), 3.98–3.94 (m, 1H), 3.47–3.37 (m, 2H), 2.36 (s, 3H), 1.68–1.61 (m, 1H), 1.57–1.47 (m, 3H), 1.37–1.27 (m, 2H), 1.20 (d, J = 7.25 Hz, 3H). ^{13}C NMR (DMSO- d_6): δ = 198.78, 174.12, 171.40, 156.01, 137.02, 128.34, 127.76, 127.62, 65.39, 54.61, 47.87, 45.30, 32.82, 31.52, 26.88, 23.04, 18.44. ESI-MS (m/z): 409.19 $[M + H]^+$. Anal. ($C_{19}H_{28}N_4O_4S$) C, H, N.

(2S,4R)-N-[(2S)-6-Ethanethioylamino-1-benzylamino-1-oxohexan-2-yl]-4-hydroxypyrrolidine-1-benzylloxycarbonyl-2-carboxamide (35): 1H NMR (DMSO- d_6): rotamers A+B δ = 9.91–9.88 (m br, 1H), 8.37 (t, J = 5.99 Hz, 0.51H), 8.25 (t, J = 5.99 Hz, 0.49H), 8.15–8.13 (m, 1H), 7.38–7.20 (–Ar, 10H), 5.06–4.93 (m, 3H), 4.41–4.38 (m, 0.5H), 4.31–4.21 (m, 4.5H), 3.53–3.42 (m, 2H), 3.37–3.33 (m, 2H), 2.37 (s, 1.49H), 2.36 (s, 1.51H), 2.12–2.04 (m, 1H), 1.86–1.83 (m, 1H), 1.78–1.71 (m, 0.5H), 1.62–1.13 (m, 5.5H). ^{13}C NMR (DMSO- d_6): rotamers A+(B) δ = 198.74, 171.96 (171.71), 171.45, 154.44 (154.00), 139.29, 136.86 (136.81), 128.37, 128.20 (128.17), 127.78, 127.47 (127.44), 127.02 (126.98), 126.88 (126.69), 68.43 (67.76), 65.96 (65.79), 59.00 (58.09), 55.33 (54.88), 52.61 (52.49), 45.33 (45.24), 41.96 (41.92), 38.54, 32.77, 31.71 (31.27), 26.88 (26.80), 22.93 (22.88). ESI-MS (m/z): 541.21 $[M + H]^+$. Anal. ($C_{28}H_{36}N_4O_5S \cdot 0.03\text{hexane}$) C, H, N.

(2S)-2-(6-Phenyhexanoylamino)-6-ethanethioylamino-N-benzylhexanamide (36): 1H NMR (DMSO- d_6): 9.92 (s br, 1H), 8.37 (t, J = 5.99 Hz, 1H), 7.90 (d, J = 7.88 Hz, 1H), 7.32–7.14 (–Ar, 10H), 4.27–4.24 (m, 3H), 3.48–3.39 (m, 2H), 2.56–2.53 (m, 2H), 2.37 (s, 3H), 2.18–2.08 (m, 2H), 1.70–1.63 (m, 1H), 1.58–1.49 (m, 7H), 1.34–1.23 (m, 4H). ^{13}C NMR (DMSO- d_6): δ = 198.75, 172.17, 171.83, 142.24, 139.40, 128.22, 128.18, 128.17, 127.00, 126.66, 125.55, 52.35, 45.28, 41.91, 35.08, 35.05, 32.78, 31.72, 30.74, 28.26, 26.87, 25.08, 23.02. ESI-MS (m/z): 468.25 $[M + H]^+$. Anal. ($C_{27}H_{37}N_3O_2S$) C, H, N.

(2S)-2-(7-Phenylheptanoylamino)-6-ethanethioylamino-N-benzylhexanamide (37): 1H NMR (DMSO- d_6): 9.92 (s br, 1H), 8.37 (t, J = 6.30 Hz, 1H), 7.91 (d, J = 7.88 Hz, 1H), 7.31–7.14 (–Ar, 10H), 4.30–4.24 (m, 3H), 3.46–3.39 (m, 2H), 2.56–2.53 (m, 2H), 2.36 (s, 3H), 2.17–2.07 (m, 2H), 1.70–1.63 (m, 1H), 1.57–1.46 (m, 7H), 1.34–1.24 (m, 6H). ^{13}C NMR (DMSO- d_6): δ = 198.77, 172.24, 171.87, 142.28, 139.41, 128.22, 128.19, 128.19, 127.00, 126.67, 125.56, 52.37, 45.29, 41.92, 35.17, 35.11, 32.79, 31.69, 30.91, 28.45, 28.43, 26.87, 25.23, 23.03. ESI-MS (m/z): 482.24 $[M + H]^+$. Anal. ($C_{28}H_{39}N_3O_2S$) C, H, N.

(2S)-2-(3-Phenylpropanoylamino)-6-ethanethioylamino-N-(pyridin-3-ylamino)hexanamide (38): 1H NMR (DMSO- d_6): δ = 10.26 (s, 1H), 9.94 (s br, 1H), 8.76 (d, J = 2.21 Hz, 1H), 8.27 (dd, J = 1.58, 4.73 Hz, 1H), 8.17 (d, J = 7.88 Hz, 1H), 8.03 (dt, J = 1.58, 8.20 Hz, 1H), 7.35 (dd, J = 4.73, 8.20 Hz, 1H), 7.27–7.15 (m, 5H), 4.42–4.38 (m, 1H), 3.47–3.40 (m, 2H), 2.84–2.81 (m, 2H), 2.53–2.42 (m, 2H), 2.36 (s, 3H), 1.73–1.66 (m, 1H), 1.63–1.49 (m, 3H), 1.37–1.20 (m, 2H). ^{13}C NMR (DMSO- d_6): δ = 198.77, 171.70, 171.37, 144.12, 141.11, 140.69, 135.50, 128.19, 128.19, 126.46, 125.94,

123.72, 53.13, 45.10, 36.45, 32.88, 31.67, 30.93, 27.05, 22.85. ESI-MS (m/z): 413.18 $[M + H]^+$. Anal. ($C_{22}H_{28}N_4O_2S$) C, H, N.

(2S)-2-[3-(2-Fluorophenyl)propanoylamino]-6-ethanethioylamino-N-(pyridin-3-ylamino)hexanamide (39): 1H NMR (DMSO- d_6): δ = 10.25 (s, 1H), 9.93 (s br, 1H), 8.75 (d, J = 2.21 Hz, 1H), 8.27 (dd, J = 1.58, 4.73 Hz, 1H), 8.20 (d, J = 7.88 Hz, 1H), 8.03 (dt, J = 1.58, 8.20 Hz, 1H), 7.34 (dd, 4.73, 8.20 Hz, 1H), 7.28 (m, 1H), 7.23 (m, 1H), 7.14–7.07 (m, 2H), 4.41–4.36 (m, 1H), 3.46–3.41 (m, 2H), 2.86–2.83 (m, 2H), 2.53–2.42 (m, 2H), 2.36 (s, 3H), 1.74–1.66 (m, 1H), 1.62–1.49 (m, 3H), 1.36–1.22 (m, 2H). ^{13}C NMR (DMSO- d_6): δ = 198.79, 171.40, 171.26, 160.53 (d, J = 242.29 Hz), 144.29, 140.90, 135.53, 130.60 (d, J = 4.62 Hz), 127.98 (d, J = 8.32 Hz), 127.71 (d, J = 15.72 Hz), 126.20, 124.23 (d, J = 3.70 Hz), 123.60, 114.92 (d, J = 21.27 Hz), 53.24, 45.19, 34.99, 32.77, 31.57, 26.91, 24.16, 22.98. ESI-MS (m/z): 431.21 $[M + H]^+$. Anal. ($C_{22}H_{27}FN_4O_2S$) C, H, N.

(2S)-N-[(2S)-6-Ethanethioylamino-1-[2-(pyridin-3-yl)ethylamino]-1-oxohexan-2-yl]-pyrrolidine-1-tert-butoxycarbonyl-2-carboxamide (40): 1H NMR (DMSO- d_6) rotamers A+B: δ = 9.91 (s br, 1H), 8.41 (s, 2H), 8.02 (s br, 0.54H), 7.87–7.82 (m, 1.46H), 7.62 (m, 1H), 7.30–7.28 (m, 1H), 4.20–4.11 (m, 2H), 3.42–3.37 (m, 3H), 3.28–3.24 (m, 2H), 2.73 (t, J = 6.94 Hz, 2H), 2.36 (s, 3H), 2.10–2.02 (m, 1H), 1.77–1.70 (m, 3H), 1.61–1.13 (m, 16H). ^{13}C NMR (DMSO- d_6): rotamers A + (B) δ = 198.76, 172.18 (171.88), 171.36, 153.95 (153.29), 149.84, 147.37, 136.17, 134.75, 123.30, 78.79 (78.34), 59.50 (59.31), 52.25, 46.71 (46.47), 45.22, 32.75, 32.09 (31.97), 31.52, 30.99, 29.68, 28.10 (27.97), 26.88, 23.94, 23.04 (22.80). ESI-MS (m/z): 506.22 $[M + H]^+$. Anal. ($C_{25}H_{39}N_5O_4S$) C, H, N.

SIRT1–3 in Vitro Assay. The Fluor de Lys fluorescence assays were based on the method described in the BioMol product sheet (Enzo Life Sciences) using the BioMol KI177 substrate for SIRT1 and the KI179 substrate for SIRT2 and SIRT3. The determined K_m value of SIRT1 for KI177 was 58 μM , and the K_m of SIRT2 for KI179 was 198 μM .²⁹ The K_m of SIRT3 for KI179 was reported by BioMol to be 32 μM . The K_m values of SIRT1, SIRT2 and SIRT3 for NAD^+ were reported by BioMol to be 558 μM , 547 μM and 2 mM, respectively.

Briefly, assays were carried out using the Fluor de Lys acetylated peptide substrate at 0.7 K_m and NAD^+ (Sigma N6522 or BioMol KI282) at 0.9 K_m , recombinant GST-SIRT1/2-enzyme or recombinant His-SIRT3 and SIRT assay buffer (KI286). GST-SIRT1 and GST-SIRT2 were produced as described previously.^{39,40} His-SIRT3 (BML-SE270) was purchased from Enzo Life Sciences. The buffer, Fluor de Lys acetylated peptide substrate, NAD^+ and DMSO/compounds in DMSO (2.5 μL in 50 μL total reaction volume; DMSO from Sigma, D2650) were preincubated for 5 min at room temperature. The reaction was started by adding the enzyme. The reaction mixture was incubated for one hour at 37 °C. After that, Fluor de Lys developer (KI176) and 2 mM nicotinamide (KI283) in SIRT assay buffer (total volume 50 μL) were added, and the incubation was continued for 45 min at 37 °C. Fluorescence readings were obtained using EnVision 2104 Multilabel Reader (PerkinElmer) with excitation wavelength 370 nm and emission 460 nm.

The IC_{50} values were determined as three independent determinations giving altogether 27 data points. All the data points were included in the calculation of the best-fit value for

nonlinear curve fitting with GraphPad Prism5 (GraphPad Software, Inc.).

Cell Culture. Human retinal pigment epithelial cells (ARPE-19, obtained from ATCC, American Type Culture Collection) and SH-SY5Y neuroblastomas (DSMZ) were grown as described earlier in Huhtiniemi et al., 2011.³² A549 lung carcinoma and MCF-7 breast carcinoma cells (both from ATCC) were maintained in Dulbecco's modified Eagle medium (DMEM; Gibco) containing 10% fetal calf serum, 100 U/mL penicillin and 100 μ g/mL streptomycin at +37 °C in a humidified atmosphere of 5% CO₂/95% air.

Western Blotting. The cells were plated to 12-well plates (Nunc) at a density of 10⁵ cells/well, and the experiments were initiated after 24 h. For the analysis of p53 acetylation levels, test compounds and etoposide (Sigma) were added at the same time and incubated for 5 h before harvesting. For the analysis of α -tubulin acetylation, the cells were treated for 6 or 18 h. Acetylated p53 Western blot analysis was done as described in Huhtiniemi et al., 2011.³² For acetylated α -tubulin Western blotting, the cells were lysed into M-PER Mammalian Protein Extraction Reagent (Thermo Fisher Scientific) followed by centrifugation (20 min, 16000g, +4 °C). After electrophoretic separation in SDS-PAGE gel, the proteins were transferred onto Hybond-ECL nitrocellulose transfer membrane (GE Healthcare) and probed with mouse monoclonal acetylated α -tubulin antibody (T6793, Sigma) and total α -tubulin antibody (T5168, Sigma). The protein signals were visualized with peroxidase-conjugated sheep anti-mouse secondary antibody (NXA931, GE Healthcare), and ECL Plus chemiluminescent substrate (GE Healthcare). The images were obtained by the use of digital imaging (ImageQuant, GE Healthcare).

Lactate Dehydrogenase Assay. Lactate dehydrogenase (LDH) leakage from the cells to medium was used as a marker for cytotoxicity. LDH was measured from cell culture medium with CytoTox assay (Promega #G1780).

Cell Proliferation and Cell Cycle Analysis. For cell proliferation assays with sulforhodamine B, A549 and MCF-7 cells were plated to 96-well plates (Nunc) 24 h before the start of the treatments (3000 cells/well). The cells were treated with vehicle (0.5% DMSO) or test compounds for 48 h (A549 cells) or 72 h (MCF-7 cells). Sulforhodamine B staining was performed as previously described.^{41,42} After treatments, 50 μ L of 50% trichloroacetic acid (Sigma) was added to each well and incubated for 1 h at +4 °C. The plates were then washed with water and air-dried. The fixed cells were incubated with 100 μ L of 0.4% sulforhodamine B solution (Sigma) at room temperature for 1 h. The plates were again washed with water and air dried, followed by solubilization of the bound dye with 200 μ L of 10 mM Tris base solution. The results were measured with EnVision plate reader (PerkinElmer) at a wavelength of 565 nm. Cell cycle analysis of A549 and MCF-7 cells was done by propidium iodide staining as previously described.⁴³ The cells were plated to 6-well plates (Nunc) 6 h before the start of the treatments (0.6 \times 10⁵ cells/well). The cells were treated with vehicle (0.5% DMSO) or test compounds for 18 h. Both adherent and floating cells were harvested and fixed with ice-cold 70% ethanol. After overnight incubation at +4 °C, the cells were collected by centrifugation and incubated with 150 μ g/mL DNase free RNase (Thermo Scientific) for 1 h at +50 °C. Propidium iodide (Sigma) was added to the final concentration of 8 μ g/mL, and incubation was continued for 2 h at +37 °C. FACScanto II flow cytometer

with FACSDiva software (Becton Dickinson) was used to analyze cellular DNA content and cell cycle.

Molecular Modeling. Homology models for SIRT1 and SIRT2 were built in bioactive conformation using the crystal structure of SIRT3 (PDB code 3glr)⁴⁴ in which is cocrystallized AceCS2-K^{Ac} peptide (⁶³⁹RSKG^{Ac}VMR) sequence, containing acetylated lysine 642 that has been identified to be deacetylated by SIRT3. The amino acid sequence of *Homo sapiens* SIRT1 and SIRT2 was obtained from the NCBI (National Center for Biotechnology Information). The sequences of SIRT1 and SIRT2 were manually aligned with SIRT3 on the basis of sequence similarity, (40% and 52.9%, respectively for the alignments, see Supporting Information).⁴⁴ Homology models for the catalytic deacetylase core of SIRT1 (555 residues) and a full-length, homology modeled SIRT2 (352 residues) was constructed using ORCHESTRA in SYBYL 1.3. The geometry of the side chains was manually optimized to obtain a crude model. The models were polished with Protein Preparation Wizards available in the Schrödinger Suite 2009.⁴⁵ In that process the bond orders were assigned, and hydrogens were added. In addition, the exhaustive sampling method was used to optimize the H-bonding and determine the orientations of hydroxyl groups, amide groups of Asn and Gln amino acids, and the proper state and orientations of the histidine imidazole rings. To relax the structure of the initial SIRT1 and SIRT2 models, the models were subjected to a restrained minimization using OPLS2001 force field, with a 0.3 Å rmsd atom displacement limit. The protein geometry was evaluated by Ramachandran plot and Verify 3D.⁴⁶ The pseudopeptidic database was prepared using Ligprep (version 2.3),⁴⁷ the geometric optimization was carried out using OLPS2005 forcefield, and all possible ionization and tautomeric forms were created at pH 8.0 \pm 0.2 using EPIK.^{48,49} The chiralities specified in the input structures were retained. Dockings were performed using Glide (version 5.5).⁵⁰ For the grid file and docking parameters were applied settings previously published by Huhtiniemi et al.³² The figures were prepared using MOE (version 2011.10).³⁴

■ ASSOCIATED CONTENT

⑤ Supporting Information

Detailed experimental procedures for synthesis and elemental analysis data and procedures for molecular modeling and the most representative docking poses. This material is available free of charge via the Internet at <http://pubs.acs.org>.

■ AUTHOR INFORMATION

Corresponding Author

*Tel.: +358 40 355 2460. Fax: +358 17 162424. E-mail: Elina.Jarho@uef.fi.

Notes

The authors declare no competing financial interest.

■ ACKNOWLEDGMENTS

We deeply thank Dr. Barbara Di Rienzo for mentoring Paolo Mellini; and Miia Reponen, Sari Ukkonen, Tiina Koivunen and M.Sc. Marko Lehtonen for their skillful assistance; and the CIMO Centre for International Mobility and Academy of Finland (Grants No. 127062 and 137788) for financial support. This work is part of COST Action TD0905: "Epigenetics: Bench to Bedside". The CSC-IT Center of Science Limited is acknowledged for providing software licenses.

■ ABBREVIATIONS USED

A549, lung cancer cell line; AceCS1/2, acetyl-CoA synthetase 1/2; ADP, adenosine diphosphate; ARPE-19, human retinal pigment epithelial cells; Boc, *tert*-butoxycarbonyl; Cbz, carbonyloxybenzyl; DMEM, Dulbecco's modified Eagle medium; DMSO, dimethyl sulfoxide; FOXO, forkhead box class O; HDAC, histone deacetylase; LDH, lactate dehydrogenase; LXR, liver X receptor; MCF-7, breast cancer cell line; NAD, nicotinamide adenine dinucleotide; NF- κ B, nuclear factor- κ B; PGC-1 α , peroxisome proliferator-activated receptor γ coactivator; SH-SY5Y, human-derived neuroblastoma cell line; SIRT, silent information regulator; TBTU, O-(benzotriazol-1-yl)-N,N,N',N'-tetramethyluronium tetrafluoroborate

■ REFERENCES

- (1) Michan, S.; Sinclair, D. Sirtuins in mammals: insights into their biological function. *Biochem. J.* **2007**, *404*, 1–13.
- (2) Hawse, W. F.; Wolberger, C. Structure-based mechanism of ADP-ribosylation by sirtuins. *J. Biol. Chem.* **2009**, *284*, 33654–33661.
- (3) He, B.; Du, J.; Lin, H. Thiosuccinyl peptides as Sirt5-specific inhibitors. *J. Am. Chem. Soc.* **2012**, *134*, 1922–1925.
- (4) Madsen, A. S.; Olsen, C. A. Substrates for efficient fluorometric screening employing the NAD-dependent sirtuin 5 lysine deacylase (KDAC) enzyme. *J. Med. Chem.* **2012**, *55*, 5582–5590.
- (5) Mostoslavsky, R.; Esteller, M.; Vaquero, A. At the crossroad of lifespan, calorie restriction, chromatin and disease: Meeting on sirtuins. *Cell Cycle* **2010**, *9*, 1907–1912.
- (6) Taylor, D. M.; Maxwell, M. M.; Luthi-Carter, R.; Kazantsev, A. G. Biological and potential therapeutic roles of sirtuin deacetylases. *Cell. Mol. Life. Sci.* **2008**, *65*, 4000–4018.
- (7) Haigis, M. C.; Sinclair, D. A. Mammalian sirtuins: Biological insights and disease relevance. *Annu. Rev. Pathol.: Mech. Dis.* **2010**, *5*, 253–295.
- (8) Guarente, L. Sirtuins as potential targets for metabolic syndrome. *Nature* **2006**, *444*, 868–874.
- (9) Xu, F.; Gao, Z.; Zhang, J.; Rivera, C. A.; Yin, J.; Weng, J.; Ye, J. Lack of SIRT1 (mammalian sirtuin 1) activity leads to liver steatosis in the SIRT1 \pm mice: A role of lipid mobilization and inflammation. *Endocrinology* **2010**, *151*, 2504–2514.
- (10) Pasco, M. Y.; Rotili, D.; Altucci, L.; Farina, F.; Rouleau, G. A.; Mai, A.; Neri, C. Characterization of sirtuin inhibitors in nematodes expressing a muscular dystrophy protein reveals muscle cell and behavioral protection by specific sirtinol analogues. *J. Med. Chem.* **2010**, *53*, 1407–1411.
- (11) Jung-Hynes, B.; Nihal, M.; Zhong, W.; Ahmad, N. Role of sirtuin histone deacetylase SIRT1 in prostate cancer: A target for prostate cancer management via its inhibition? *J. Biol. Chem.* **2009**, *284*, 3823–3832.
- (12) Huffman, D. M.; Grizzle, W. E.; Bamman, M. M.; Kim, J.; Eltoum, I. A.; Elgavish, A.; Nagy, T. R. Sirt1 is significantly elevated in mouse and human prostate cancer. *Cancer Res.* **2007**, *67*, 6612–6618.
- (13) Bradbury, C. A.; Khanim, F. L.; Hayden, R.; Bunce, C. M.; White, D. A.; Drayson, M. T.; Craddock, C.; Turner, B. M. Histone deacetylases in acute myeloid leukemia show a distinctive pattern of expression that changes selectively in response to deacetylase inhibitors. *Leukemia* **2005**, *19*, 1751–1759.
- (14) Kozako, T.; Aikawa, A.; Shoji, T.; Fujimoto, T.; Yoshimitsu, M.; Shirasawa, S.; Tanaka, H.; Honda, S. I.; Shimeno, H.; Arima, N.; Soeda, S. High expression of the gene product SIRT1 and apoptosis induction by sirtinol in adult T-cell leukemia cells. *Int. J. Cancer* **2012**, *131*, 2044–2055.
- (15) Stunkel, W.; Peh, B. K.; Tan, Y. C.; Nayagam, V. M.; Wang, X.; Saltotellez, M.; Ni, B. H.; Entzeroth, M.; Wood, J. Function of the SIRT1 protein deacetylase in cancer. *Biotechnol. J.* **2007**, *2*, 1360–1368.
- (16) Elangovan, S.; Ramachandran, S.; Venkatesan, N.; Ananth, S.; Gnana-Prakasam, J. P.; Martin, P. M.; Browning, D. D.; Schoenlein, P. V.; Prasad, P. D.; Ganapathy, V.; Thangaraju, M. SIRT1 is essential for oncogenic signaling by estrogen/estrogen receptor α in breast cancer. *Cancer Res.* **2011**, *71*, 6654–6664.
- (17) Sun, Y.; Sun, D.; Li, F.; Tian, L.; Li, C.; Li, L.; Lin, R.; Wang, S. Downregulation of Sirt1 by antisense oligonucleotides induces apoptosis and enhances radiation sensitization in A549 lung cancer cells. *Lung Cancer* **2007**, *58*, 21–29.
- (18) Di Marcotullio, L.; Canettieri, G.; Infante, P.; Greco, A.; Gulino, A. Protected from the inside: Endogenous histone deacetylase inhibitors and the road to cancer. *Biochim. Biophys. Acta, Rev. Cancer* **2011**, *1815*, 241–252.
- (19) Jin, Y. H.; Kim, Y. J.; Kim, D. W.; Baek, K. H.; Kang, B. Y.; Yeo, C. Y.; Lee, K. Y. Sirt2 interacts with 14–3-3 β /gamma and down-regulates the activity of p53. *Biochem. Biophys. Res. Commun.* **2008**, *368*, 690–695.
- (20) Alhazzazi, T. Y.; Kamarajan, P.; Joo, N.; Huang, J. Y.; Verdin, E.; D'Silva, N. J.; Kapila, Y. L. Sirtuin-3 (SIRT3), a novel potential therapeutic target for oral cancer. *Cancer* **2011**, *117*, 1670–1678.
- (21) Peck, B.; Chen, C. Y.; Ho, K. K.; Di Fruscia, P.; Myatt, S. S.; Coombes, R. C.; Fuchter, M. J.; Hsiao, C. D.; Lam, E. W. SIRT inhibitors induce cell death and p53 acetylation through targeting both SIRT1 and SIRT2. *Mol. Cancer Ther.* **2010**, *9*, 844–855.
- (22) Lain, S.; Hollick, J. J.; Campbell, J.; Staples, O. D.; Higgins, M.; Aoubala, M.; McCarthy, A.; Appleyard, V.; Murray, K. E.; Baker, L.; Thompson, A.; Mathers, J.; Holland, S. J.; Stark, M. J.; Pass, G.; Woods, J.; Lane, D. P.; Westwood, N. J. Discovery, in vivo activity, and mechanism of action of a small-molecule p53 activator. *Cancer Cell* **2008**, *13*, 454–463.
- (23) Rotili, D.; Tarantino, D.; Carafa, V.; Lara, E.; Meade, S.; Botta, G.; Nebbioso, A.; Schemies, J.; Jung, M.; Kazantsev, A. G.; Esteller, M.; Fraga, M. F.; Altucci, L.; Mai, A. Identification of tri- and tetracyclic pyrimidinediones as sirtuin inhibitors. *ChemMedChem.* **2010**, *5*, 674–677.
- (24) Rotili, D.; Tarantino, D.; Nebbioso, A.; Paolini, C.; Huidobro, C.; Lara, E.; Mellini, P.; Lenoci, A.; Pezzi, R.; Botta, G.; Lahtela-Kakkonen, M.; Poso, A.; Steinkühler, C.; Gallinari, P.; De Maria, R.; Fraga, M.; Esteller, M.; Altucci, L.; Mai, A. Discovery of salermide and related sirtuin inhibitors: Binding mode studies and antiproliferative effects in cancer cells including cancer stem cells. *J. Med. Chem.* **2012**, *55*, 10937–10947.
- (25) Fatkins, D. G.; Monnot, A. D.; Zheng, W. N $^{\epsilon}$ -Thioacetyl-lysine: A multi-facet functional probe for enzymatic protein lysine N $^{\epsilon}$ -deacetylation. *Bioorg. Med. Chem. Lett.* **2006**, *15*, 3651–3656.
- (26) Smith, B. C.; Denu, J. M. Acetyl-lysine analog peptides as mechanistic probes of protein deacetylases. *J. Biol. Chem.* **2007**, *282*, 37256–37265.
- (27) Smith, B. C.; Denu, J. M. Mechanism-Based inhibition of Sir2 deacetylases by thioacetyl-lysine peptide. *Biochemistry* **2007**, *46*, 14478–14486.
- (28) Smith, B. C.; Hallows, W. C.; Denu, J. M. Mechanisms and molecular probes of sirtuins. *Chem. Biol.* **2008**, *15*, 1002–1013.
- (29) Kiviranta, P. H.; Suuronen, T.; Wallen, E. A. A.; Leppänen, J.; Tervonen, J.; Kyrylenko, S.; Salminen, A.; Poso, A.; Jarho, E. M. N $^{\epsilon}$ -Thioacetyl-lysine-containing tri-, tetra-, and pentapeptides as SIRT1 and SIRT2 inhibitors. *J. Med. Chem.* **2009**, *52*, 2153–2156.
- (30) Huhtiniemi, T.; Suuronen, T.; Lahtela-Kakkonen, M.; Bruijn, T.; Jääskeläinen, S.; Poso, A.; Salminen, A.; Leppänen, J.; Jarho, E. N $^{\epsilon}$ -Modified lysine containing inhibitors for SIRT1 and SIRT2. *Bioorg. Med. Chem.* **2010**, *18*, 5616–5625.
- (31) Suzuki, T.; Asaba, T.; Imai, E.; Tsumoto, H.; Nakagawa, H.; Miyata, N. Identification of a cell-active non-peptide sirtuin inhibitor containing N-thioacetyl lysine. *Bioorg. Med. Chem. Lett.* **2009**, *19*, 5670–5672.
- (32) Huhtiniemi, T.; Salo, H. S.; Suuronen, T.; Poso, A.; Salminen, A.; Leppanen, J.; Jarho, E.; Lahtela-Kakkonen, M. Structure-based design of pseudopeptidic inhibitors for SIRT1 and SIRT2. *J. Med. Chem.* **2011**, *54*, 6456–6468.

- (33) Ashworth, I. W.; Cox, B. G.; Meyrick, B. Kinetics and mechanism of N-Boc cleavage: evidence of a second-order dependence upon acid concentration. *J. Org. Chem.* **2010**, *75*, 8117–8125.
- (34) *Molecular Operating Environment (MOE)*, 2011.10; Chemical Computing Group Inc.: Montreal, QC, Canada, 2011.
- (35) Bhattacharya, S.; Chaum, E.; Johnson, D. A.; Johnson, L. R. Age-related susceptibility to apoptosis in human retinal pigment epithelial cells is triggered by disruption of p53-Mdm2 association. *Invest. Ophthalmol. Visual Sci.* **2012**, *53*, 8350–8366.
- (36) Wu, Y.; Li, X.; Zhu, J. X.; Xie, W.; Le, W.; Fan, Z.; Jankovic, J.; Pan, T. Resveratrol-activated AMPK/SIRT1/autophagy in cellular models of Parkinson's disease. *Neurosignals* **2011**, *19*, 163–174.
- (37) Solomon, J. M.; Pasupuleti, R.; Xu, L.; McDonagh, T.; Curtis, R.; DiStefano, P. S.; Huber, L. J. Inhibition of SIRT1 catalytic activity increases p53 acetylation but does not alter cell survival following DNA damage. *Mol. Cell. Biol.* **2006**, *26*, 28–38.
- (38) Peck, B.; Chen, C. Y.; Ho, K. K.; Di Fruscia, P.; Myatt, S. S.; Coombes, R. C.; Fuchter, M. J.; Hsiao, C. D.; Lam, E. W. SIRT inhibitors induce cell death and p53 acetylation through targeting both SIRT1 and SIRT2. *Mol. Cancer Ther.* **2010**, *9*, 844–855.
- (39) Kiviranta, P. H.; Leppänen, J.; Rinne, V. M.; Suuronen, T.; Kyrylenko, O.; Kyrylenko, S.; Kuusisto, E.; Tervo, A. J.; Järvinen, T.; Salminen, A.; Poso, A.; Wallén, E. A. A. N-(3-(4-Hydroxyphenyl)-propenyl)-amino acid tryptamides as SIRT2 inhibitors. *Bioorg. Med. Chem. Lett.* **2007**, *17*, 2448–2451.
- (40) Tervo, A. J.; Kyrylenko, S.; Niskanen, P.; Salminen, A.; Leppänen, J.; Nyronen, T. H.; Järvinen, T.; Poso, A. An in silico approach to discovering novel inhibitors of human sirtuin type 2. *J. Med. Chem.* **2004**, *47*, 6292–6298.
- (41) Shoemaker, R. H. The NCI60 human tumour cell line anticancer drug screen. *Nat. Rev. Cancer* **2006**, *6*, 813–823.
- (42) Peck, B.; Chen, C. Y.; Ho, K. K.; Di Fruscia, P.; Myatt, S. S.; Coombes, R. C.; Fuchter, M. J.; Hsiao, C. D.; Lam, E. W. SIRT inhibitors induce cell death and p53 acetylation through targeting both SIRT1 and SIRT2. *Mol. Cancer Ther.* **2010**, *9*, 844–855.
- (43) Nuutinen, U.; Ropponen, A.; Eeva, J.; Eray, M.; Pellinen, R.; Wahlfors, J.; Pelkonen, J. The effect of microenvironmental CD40 signals on TRAIL- and drug-induced apoptosis in follicular lymphoma cells. *Scand. J. Immunol.* **2009**, *70*, 565–573.
- (44) Jin, L.; Wei, W.; Jiang, Y.; Peng, H.; Cai, J.; Mao, C.; Dai, H.; Choy, W.; Bemis, J. E.; Jirousek, M. R.; Milne, J. C.; Westphal, C. H.; Perni, R. B. Crystal structures of human SIRT3 displaying substrate-induced conformational changes. *J. Biol. Chem.* **2009**, *284*, 24394–24405.
- (45) *Schrödinger Suite 2009 Protein Preparation Wizard*; Schrödinger, LLC: New York, NY, 2009.
- (46) *Verify3D Structure Evaluation Server*: http://nihserver.mbi.ucla.edu/Verify_3D/
- (47) *Lig Prep*, version 2.3; Schrödinger, LLC: New York, NY, 2009.
- (48) *Epik*, version 2.2, Schrödinger, LLC, New York, NY, 2011.
- (49) Shelley, J. C.; Cholleti, A.; Frye, L. L.; Greenwood, J. R.; Timlin, M. R.; Uchiyama, M. Epik: A software program for pK_a prediction and protonation state generation for drug-like molecules. *J. Comput.-Aided. Mol. Des.* **2007**, *21*, 681–691.
- (50) *Glide*, version 5.5; Schrödinger, LLC: New York, NY, 2009.